ESC-TR-95-021

Technical Report 1022

A Metric Analysis of IRAS Resident Space Object Detections

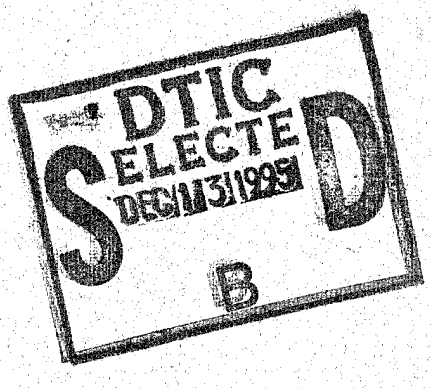

M.T. Lane
J.F. Baldassini
E.M. Gaposchkin

1 November 1995

Lincoln Laboratory
MASSACHUSETTS INSTITUTE OF TECHNOLOGY
LEXINGTON, MASSACHUSETTS

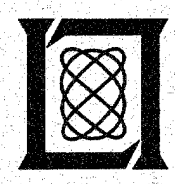

Prepared for the Ballistic Missile Defense Organization
under Air Force Contract F19628-95-C-0002.

Approved for public release; distribution is unlimited.

19951211 069

DTIC QUALITY INSPECTED 1

This report is based on studies performed at Lincoln Laboratory, a center for research operated by Massachusetts Institute of Technology. The work was sponsored by the Ballistic Missile Defense Organization under Air Force Contract F19628-95-C-0002.

This report may be reproduced to satisfy needs of U.S. Government agencies.

The ESC Public Affairs Office has reviewed this report, and it is releasable to the National Technical Information Service, where it will be available to the general public, including foreign nationals.

This technical report has been reviewed and is approved for publication.

FOR THE COMMANDER

Gary Tutungian
Administrative Contracting Officer
Contracted Support Management

Non-Lincoln Recipients

PLEASE DO NOT RETURN

Permission is given to destroy this document when it is no longer needed.

MASSACHUSETTS INSTITUTE OF TECHNOLOGY
LINCOLN LABORATORY

A METRIC ANALYSIS OF IRAS RESIDENT SPACE OBJECT DETECTIONS

M.T. LANE
J.F. BALDASSINI
E.M. GAPOSCHKIN
Group 91

TECHNICAL REPORT 1022

1 NOVEMBER 1995

Approved for public release; distribution is unlimited.

LEXINGTON MASSACHUSETTS

ABSTRACT

The Infrared Astronomy Satellite (IRAS) was launched and operated during a 10-month period in 1983. The orbit was close to the MSX orbit design, but the science data were collected in a mode where the focal plane was pointing directly away from the Earth. Using the raw data tapes, the Space Research Institute at Groningen, Netherlands, collected approximately 139,000 tracks of data that had focal plane motion different than astronomical sources, and the IRAS Processing and Analysis Center (IPAC) determined the boresite pointing of IRAS to within 20 arcsec. This report will focus on the nonastronomical detections from IRAS, many of which are Resident Space Objects (RSOs). In particular, the focus of the study is on how many are correlated to the known RSO catalogue for 1983 and the calibration and characterization of the metric accuracy for the correlated data. This study was undertaken to prepare for analysis of RSO detections from the MSX satellite and, in particular, so that automatic analysis tools designed for analysis of surveillance experiment data could be tested. The supporting analysis tools, required corollary data, and metric calibration procedure will be described, and the results of the accuracy of the IRAS ephemeris and metric RSO detections will be presented.

Accession For
NTIS GRA&I ☑
DTIC TAB ☐
Unannounced ☐
Justification
By
Distribution/
Availability Codes
Dist | Avail and/or Special

TABLE OF CONTENTS

LIST OF ILLUSTRATIONS

LIST OF TABLES

1. INTRODUCTION

The Infrared Astronomy Satellite (IRAS) was launched in early 1983 and operated for a 10-month period to collect repeated observations of the star background in four infrared wavelengths: 12, 25, 60, and 100 μ. The orbit was selected to be near-circular with a 103-min period close to a sun-synchronous inclination of 99 deg. IRAS always pointed its focal plane away from the Earth and used a scan rate of 3.85 arcmin/s, which is slightly faster than the orbital motion. This way a stellar point source will go through several detectors during a typical scan.

Processing of the IRAS raw data (aimed at extracting all inertially fixed point source detections) was carried out at the IRAS Processing and Analysis Center (IPAC) at the Jet Propulsion Laboratory (JPL) and involved three aspects of a metric screening process: a "Seconds Confirmation" test, an "Hours Confirmation" test, and a "Weeks Confirmation" test. The Seconds Confirmation test verified that a point source traveled across the IRAS focal plane during a scan at the predicted rate (3.85 arcmin/s) and in the predicted (in-scan or "image") direction. The success of this test indicated that the point source was a large distance away from the IRAS platform and was probably astronomical in nature. The Hours Confirmation test verified that the point source was observed again after a full orbit of IRAS was completed and the focal plane was looking in the same part of the sky as before. This test indicated that the point source is moving very slowly with respect to the IRAS focal plane and is probably a very large distance away. The Weeks Confirmation test was used when (after several weeks) IRAS was again directed to look in the same part of the sky as the first detections. IRAS was designed to repeat coverage of the sky three times during the 10-month mission. About 96% of the sky was visited at least twice, and about 76% of the sky was visited a third time. If the Seconds, Hours, and Weeks Confirmation tests were all passed, then the point source was considered to be inertially fixed upon the sky. Those that fail the Weeks Confirmation test can be asteroids or some other astronomical point source at a large distance from the IRAS focal plane, and those that fail the Hours test can be faster-moving asteroids, pieces from comets, or other space debris particles. Those that fail the Seconds Confirmation test (that is, they have a focal plane rate different than 3.85 arcmin/s and in possibly a different direction than the in-scan direction) are possibly artificial Earth satellites, known as Resident Space Objects (RSOs), and can be close to the IRAS focal plane. An onboard procedure attempted to preclude data on particles or infrared sources very close to the IRAS focal plane, and therefore, if an RSO was observed by IRAS, it would typically be seen at a range of 1000 km or greater.

The potential RSO observations from this last category of point sources become the focus of this study, and several questions are to be addressed. First, how many of these potential RSOs were observed by IRAS, and how many are correlated to the known RSO catalogue from 1983? Second, what is the metric accuracy of the correlated RSO detections and metric error budget for the reduced data, and how can the metric data be calibrated? Third, how reliable are the uncorrelated detections to provide an observed sample of the 1983 debris population?

This study was undertaken to prepare for analysis of surveillance experiment data from the Midcourse Space Experiment (MSX) satellite program [1]. The MSX is scheduled for launch in 1995 and is a space flight program designed, in part, to demonstrate surveillance of space and the RSO background from space. The technical challenges include cryogenic technology for cooling an infrared sensor: low-

noise, high-performance focal planes; high, off-axis, stray-light rejection optics; on-orbit signal processing and data compression; and contamination control. The orbit is specified to be 900-km altitude, circular, at nearly a sun-synchronous inclination of 99.23 deg. The lifetime of the infrared sensor is expected to be 20 months, and the visible and ultraviolet sensors have a planned operation period of 60 months. The infrared sensor has a five-band scanning radiometer (from 4.3 to 26 μ) with a 14-in telescope. The pixel size is 90 μrad, and there will be an onboard signal and data processor for compression and data processing. The IRAS nonastronomical data become a real space-based data source for testing the automatic analysis tools designed for MSX RSO detections, and all facets of the analysis are involved. The suite of test data from IRAS includes potential RSO detections from the IRAS sensor, a precise ephemeris for the IRAS platform, and supporting corollary data such as a catalogue of RSO element sets updated for each observation day of 1983 and independent metric observations on each RSO that IRAS observed. Each of these aspects of the analysis will be described, and the calibration of the IRAS detections and results from an automatic analysis of the data will be presented.

2. CALIBRATED IRAS METRIC OBSERVATIONS

2.1 REDUCTION OF FOCAL PLANE DETECTIONS TO INERTIAL COORDINATES

Detected point sources that could be potential observations of RSOs are those that have different (and often faster) focal plane motion from the scan rate of 3.85 arcmin/s. Often these sources will also have a focal plane direction different from the in-scan direction, although this is not a necessary condition. The Seconds, Hours, and Weeks Confirmation tests were designed to glean from the "hundreds of thousands of detections per day" the inertially fixed sources [2], and in this way a series of metric tests can be used. In this current study, however, where the sources are not inertially fixed upon the sky, there is no metric test that can indicate whether the detections are noise, radiation hits or infrared sources near (or from) the spacecraft (such as material emitted by IRAS itself), or actual RSOs. The Space Research Institute at Groningen, Netherlands, collected approximately 139,000 tracks of IRAS data (involving nearly 520,000 individual detections) that satisfied the following properties: (a) the focal plane motion was different than the 3.85 arcmin/s scan rate, (b) the timing of three or more detector hits was consistent with a single in-scan velocity, and (c) each detector had an observed flux value of 0.1 Jy or more [3]. This data base, referred to as the "debris data base," was designed to capture all possible RSO detections (and in particular debris measurements). The debris data base used the raw IRAS data (at IPAC), and for each track that passed the above criteria, the following data were provided: the absolute time a track passed a line through the boresite perpendicular to the image direction, the flux value and detector identification for each detection recorded, and the in-scan velocity across the focal plane. No 100-μ detector values were included in the debris data base.

Figure 2.1 (extracted from Beichman et al. [2]) displays the focal plane detector suite. The absolute time given with each track is when the streak crosses the imaginary vertical line going through the boresite (denoted by the + symbol). Note that a detector can be up to 4.75 arcmin long and up to 1.51 arcmin wide. For this study, absolute time and position in the focal plane for each observation from a detector are required, and therefore the following calibration of the data from the debris data base was performed. The center of each detector belonging to a track was selected for a set of initial points, and a line was fit in a least-squares fashion to these positions. If the line went through a lit detector, then the calibrated focal plane position was taken to be the point on the line halfway through the detector on the line. If the line was off of the detector, then the nearest corner of the detector was chosen as the focal plane position. With the in-scan velocity provided in the data base, the relative time of the observed point on a detector was determined by calculating the distance of the point to the absolute reference time line along the track and dividing by the in-scan velocity. This method provides the number of seconds from the absolute reference time, and the absolute time of each detection in the track can thereby be determined. The image direction is perpendicular to the ecliptic plane, and therefore the declination direction is skewed from the image direction by the inclination of the ecliptic. Figure 2.1 shows that the image direction is horizontal from right to left. The right ascension direction is skewed from the cross-scan direction by the same amount, and since the detectors are longest in the right ascension direction and no information is contained in the data base concerning the resolution of an observation on a detector, the right ascension measurements can be more noisy than the declination due to the uncertainty of the position on the detector in the cross-scan direction.

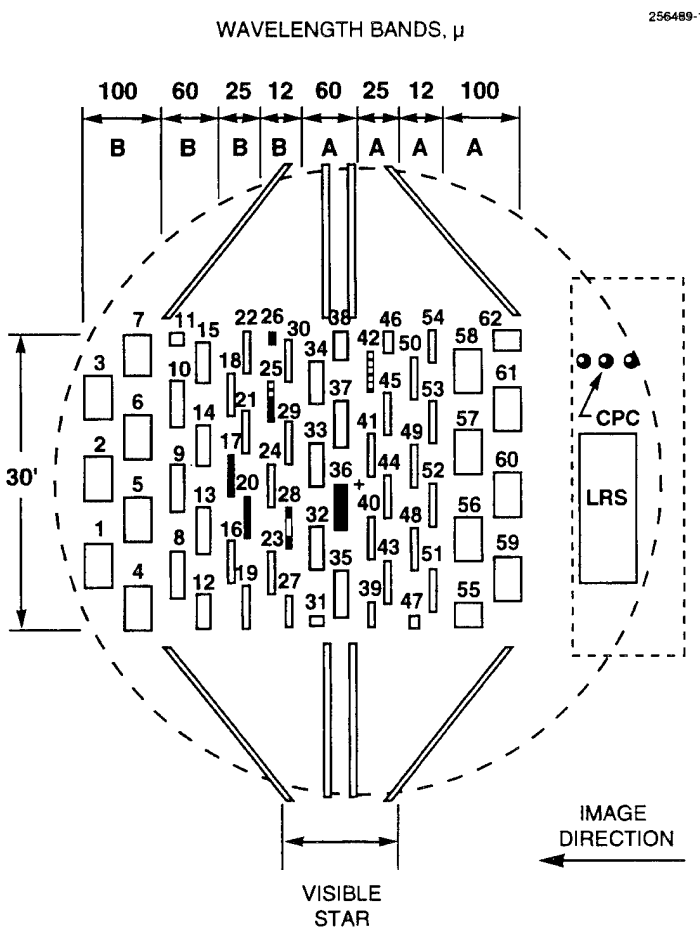

Figure 2.1. The IRAS focal plane and suite of detectors (from Beichman et al. [2]).

An example of an IRAS track and the calibration procedure described is presented below. Table 2.1 gives relevant data pertaining to IRAS Track #664140. (The IRAS Track ID numbers listed here are artificial designators and do not correspond to other listings.) This track was collected on Day 258 of 1983, and an in-scan velocity of 4.46 arcmin/s was recorded. Table 2.1 shows that there were eight detections involved in the track, and for each detection the following data are given: time from the first detection, detector number, wavelength of the detector, the recorded flux (in Janskys), the calibrated position in the X (or cross-scan) and Y (or image) directions, and the boundaries of the detector in the X and Y directions. Position units are given in arcminutes on the focal plane from the boresite. The position data are plotted in Figure 2.2, where the graph has been oriented in a similar fashion to the map of the focal plane in Figure 2.1. The center of each detector is highlighted by the triangle symbol, and the calibration positions

are denoted by squares. Note that the curve fit to the calibrated positions is not a straight line since a line fit to the centers of the detectors would not go completely through Detectors 54 and 18. In these instances, the edge of the detectors are chosen as the calibrated focal plane positions.

TABLE 2.1

An Example IRAS Track (#664140) with Relevant Focal Plane Position Data

#	TIME (s)	DET #	BAND	Jy	XPOS	YPOS	X1	X2	Y1	Y2
1	0.000	54	I12	1.55	−11.73	−7.80	−15.09	−11.73	−7.80	−7.04
2	0.484	50	I12	2.15	−11.27	−5.66	−11.96	−7.41	−6.04	−5.28
3	1.498	42	I25	2.10	−11.20	−1.14	−13.10	−8.45	−1.52	−0.76
4	2.782	34	I60	1.05	−11.11	4.59	−12.10	−7.35	3.84	5.35
5	3.482	30	I12	2.12	−11.06	7.71	−14.08	−9.63	7.33	8.09
6	4.505	22	I25	0.21	−10.99	12.27	−15.12	−10.64	11.89	12.65
7	4.987	18	I25	2.50	−10.95	14.42	−10.94	−6.29	13.66	14.42
8	5.610	15	I60	0.20	−10.92	17.20	−14.23	−9.48	16.45	17.96
Track ID: 664140 Year: 1983 Day: 258.570484375 In-Scan Velocity: 4.46 (Arcmin/s)										

Once the absolute focal plane position for each IRAS detection is determined, calibrated boresite pointing data are used to transform the data to inertial right ascension and declination measurements. Figure 2.3 (extracted from Beichman et al. [2]) shows the IRAS control axes with respect to the sun. The Y axis is the boresite axis with the angle ψ determining the scan rate. The angle θ completes the orientation of the focal plane in this reference system. During a viewing scenario, θ remained roughly constant, and ψ changed in a nearly linear fashion. If ψ and θ are known, then the inertial position of any point on the focal plane can be determined by first rotating the point on the focal plane to the solar reference frame and transforming this frame to the inertial frame using the known apparent ephemeris of the sun about the Earth. These values were determined for the entire mission by IPAC as a result of an intensive analysis of the IRAS onboard attitude sensors and stars observed by IRAS. An estimated 1-sigma accuracy of these values is 10 to 20 arcsec (or 4 to 8 mdeg) [4]. IPAC supplied the pointing for each time in the debris data base.

Mathematically, if (x,y) denotes a focal plane position, and $\mathbf{w}$ denotes a unit vector in the IRAS focal plane coordinate frame $\mathbf{w} = (-x, y, z)$ (with $z^2 = 1 - x^2 - y^2$), then one can derotate the vector $\mathbf{w}$ using the boresite reference angles ψ and θ for the specified time

$$\mathbf{v} = R_3(-\theta)\, R_2(-\psi)\, \mathbf{w} \quad ,$$

and calculate angles ψ' and θ' in the sun-reference coordinate frame depicted in Figure 2.3 for the point (x,y). These angles are calculated as $\theta' = \tan^{-1}[v(2)/v(1)]$ and $\psi' = \cos^{-1}[v(3)]$ and can be transformed to the inertial coordinate frame using the position of the Sun with respect to the inertial frame.

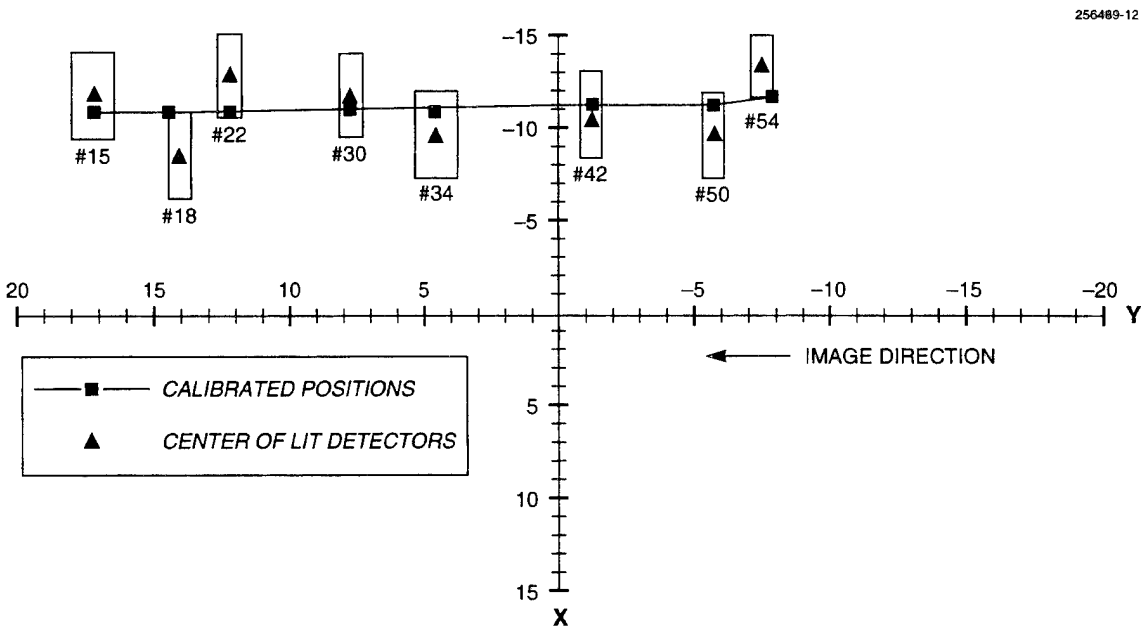

Figure 2.2. Plot of data in Table 2.1 providing an example of an RSO streak across the IRAS focal plane (units are in arcminutes).

2.2 PROBLEMS WITH REDUCTION AND SCREENING OF THE DATA

A significant problem with the way the debris data base has been collected is that if even one detector in a track is falsely lit (as is possible from the radiation sources mentioned above or because a detector is behaving in a noisy fashion), then the fit of the line to all the detections in the track can be thrown off, and the calibrated positions of each of the other detectors can be in error. In fact, this is entirely possible. Most of the detectors in the focal plane have a measured response for the mean rms noise floor of 0.15 to 0.2 Jy, and some of the detectors exhibited a measured mean rms noise value of > 0.3 Jy [2]. A histogram of the Noise Equivalent Flux Density (NEFD) of the detectors is given in Beichman et al. and reproduced below in Figure 2.4. These data were collected on-orbit to estimate the 1-sigma noise for a single sample. Since the debris data base had used a noise floor of 0.1 Jy (in the hope of gathering all the orbital debris data), it is opened up to the possibility of a large amount of spurious data with no means of screening the tracks metrically.

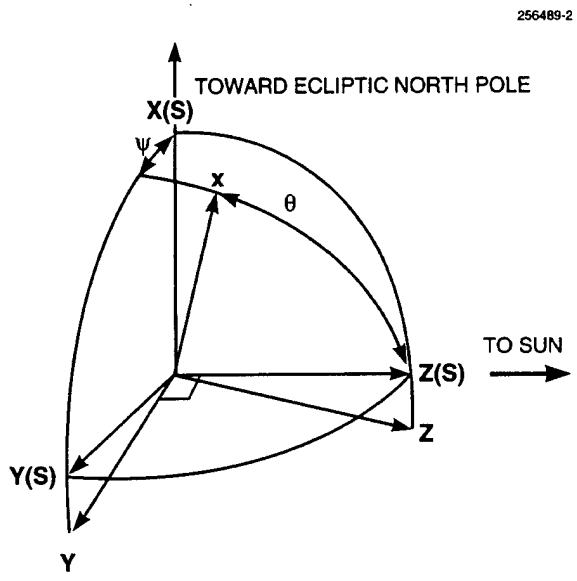

Figure 2.3. The IRAS spacecraft control axes (X,Y, and Z) as referred to the sun and North Ecliptic Pole [labeled X(S), Y(S), and Z(S)],(from [2]).

An excellent example of a track plagued by this problem is shown in Table 2.1. Detectors 22 and 15 both have flux values close to 0.2 Jy. This is dangerously close to the noise floor for both of these detectors, as shown in Figure 2.4. If these were spurious detections, then the calibration procedure plotted in Figure 2.2 would be very different for the remaining data points in the track. This would alter each of the calibrated positions as well as the in-scan velocity, which affects the absolute time. The track presented in Table 2.1 has been correlated to the known geosynchronous RSO SSC #14158, and it was observed by IRAS at a range of over 35,000 km. An independent orbit for this RSO has been calculated, and metric residuals determined by comparing the orbit with the calibrated inertial positions are shown in Table 2.2. The two low-flux detections at the end of the track could contribute to the large deviation in the position data compared to the orbit. The biases are most likely due to boresite pointing error.

Unfortunately, tracks like this example are not rare. Combinatorial statistics from the IRAS debris data base are shown in Table 2.3. More than 47% of the observations involve flux values < 0.6 Jy, and more than 77% have flux values of < 1 Jy. Moreover, more than 26% of the tracks have an in-scan velocity < 4 arcmin/s, and these tracks are more likely to be astronomical objects rather than RSOs. (The typical geosynchronous RSO will have an in-scan velocity between 4.5 and 4.6 arcmin/s.)

The noisy response functions from the detectors make it difficult to screen out bad data using the radiometric flux measurements. A 3-sigma value for confidence in the flux measurements implies that most measurements have an uncertainty of 0.6 to 1 Jy. These figures question the reliability of tracks of small-sized objects (such as debris), where flux values < 1 Jy are typical. Moreover, the sensitivity of the

detectors precludes screening tracks by temperature (as determined by ratios of flux measurements from the different wavelength passbands) since uncertainties of this level can produce temperature deviations as much as 50% for faint targets.

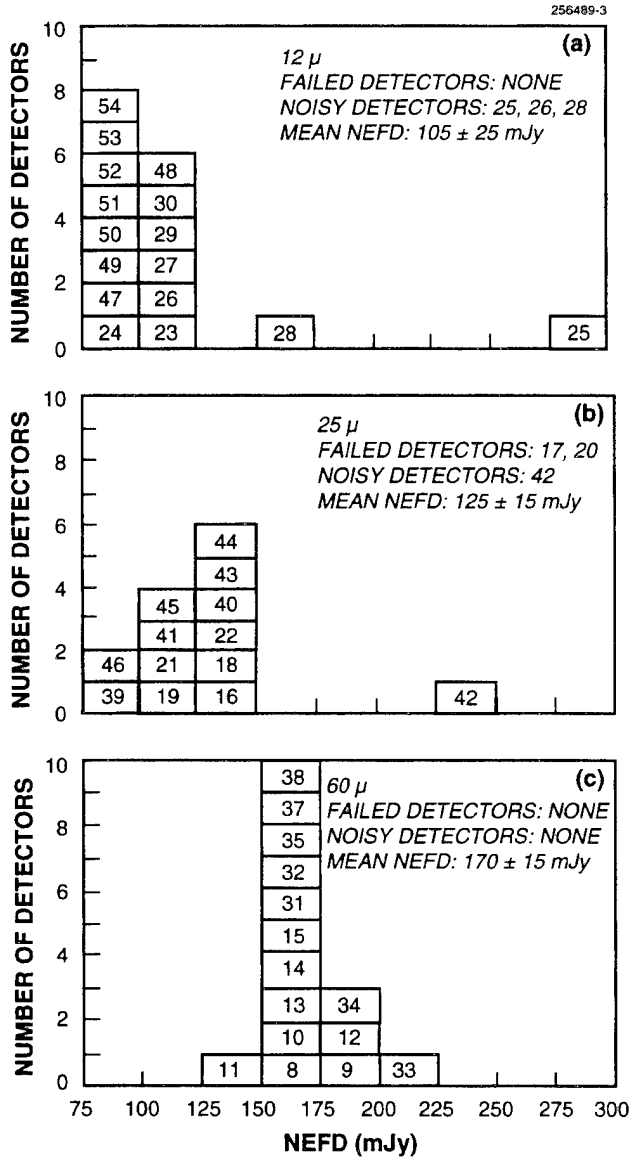

Figure 2.4. Histograms of NEFDs under quiescent conditions (from Beichman et al. [2]). The detector number is indicated in each box.

TABLE 2.2

Metric Residuals from Comparing an Independent RSO Orbit with IRAS Track #664140

IRAS Track ID	Time (sec from t0)	delta ra (mdeg)	delta dec (mdeg)
664140	0.000	−4.5	−15.5
664140	0.484	−0.5	−14.4
664140	1.498	−6.8	−13.3
664140	2.782	−14.9	−11.9
664140	3.482	−19.2	−11.2
664140	4.505	−25.6	−10.0
664140	4.987	−28.3	−9.5
664140	5.610	−32.4	−8.9

Time (Days from 1983)	Object#	ra bias	ra σ	dec bias	dec σ
258.5704843985	14158	−16.5	11.8	−11.8	2.4

TABLE 2.3

Combinatorial Statistics from the IRAS Debris Data Base

(In-scan velocity limits are given in arcmin/s and flux limits are given in Janskys)

Category	Number	Percentages
Observations (Total)	519988	
Tracks (Total)	138902	
Days	277	
Tracks with In-Scan Velocity < 4	36321	26.15%
Tracks with In-Scan Velocity ≥ 4 and < 6	41222	29.68%
Tracks with In-Scan Velocity ≥ 6	61359	44.17%
Observations with Flux Value < 0.6	244454	47.01%
Observations with Flux Value ≥ 0.6 and < 1.0	156960	30.19%
Observations with Flux Value ≥ 1.0 and < 1.5	65085	12.52%
Observations with Flux Value ≥ 1.5	53489	10.29%

It appears then that only a metric confirmation (of a track with an orbit of a known RSO) can be made on tracks containing flux values < 0.6 Jy, and observed RSOs with flux values > 1 Jy are generally bigger than small (centimeter-sized) debris. It will be demonstrated that IRAS did see a large number of known RSOs from ranges of 1000 km to the geosynchronous orbit range of 35,000 km, but one cannot say with any measure of confidence what type of debris was seen (or how many debris measurements are available).

2.3 THE METRIC ERROR BUDGET FOR THE REDUCED DATA

The timing estimate for each detection is made by estimating the response function near 1-sec boundaries and taking the absolute time to fall at the peak of the response function [2]. The error from this procedure should be no worse than 10 msec, which translates into an ephemeris error of at most 70 m. This affects the accuracy of the data in a worst-case scenario as follows: at 1000-km range, a 70-m ephemeris error will produce an observed angle error of 4 mdeg.

For tracks with no erroneous measurements, a bias in the reduced right ascension and declination measurements will be induced by the error in boresite pointing (4 to 8 mdeg). For worst-case scenarios, the standard deviation of the individual error can be up to 0.7 arcmin (12 mdeg) in the in-scan direction and up to 2.5 arcmin (42 mdeg) in the cross-scan direction. If the track contains data from four or more separate detectors, then the bias error will remain the same, but the standard deviation of the error can be smaller by a factor of 2. If there are one or more false detections in a track, then the error from a good measurement can increase to 5 arcmin (or 83 mdeg) in the cross-scan direction, but most likely these tracks will show up with large standard deviations because the track is skewed to include the erroneous data.

A summary of the metric error budget for IRAS observations is provided in Table 2.4. This table shows the error source, a worst-case estimate for the error, when the worst case can be realized, a normal-case estimate, and assumptions assumed for the normal-case error. In each category, the root of the sum of the squares (rss) of the errors is provided. Table 2.4 shows a worst-case metric error for an individual IRAS observation is 80.7 mdeg with a normal case 10.8 mdeg.

TABLE 2.4
The Metric Error Budget for IRAS RSO Observations

Error Source	Worst Case	Worst-Case Description	Normal Case	Normal-Case Description
Time Error	4.0 mdeg	10-msec error at 1000-km range	0.4 mdeg	10-msec error at > 10,000-km range
IRAS Ephemeris	5.7 mdeg	100-m error at 1000-km range	0.3 mdeg	40-m error at > 10,000-km range
Pointing Error	8.0 mdeg	upper pointing error limit	4.0 mdeg	lower pointing error limit
Focal Plane Position	80.0 mdeg	4.75-arcmin position error due to erroneous parts of the track	10.0 mdeg	1/2-arcmin position error
Total Error	80.7 mdeg		10.8 mdeg	

3. THE PRECISE IRAS PLATFORM EPHEMERIS

To perform a precise metric analysis of IRAS observations, a precise ephemeris of the IRAS platform is necessary for any time of interest. This was not a prime requirement for IPAC and for performing an analysis of inertially fixed point sources and other slowly changing astronomical data from IRAS, but a precise platform ephemeris is critical in analyzing the metric accuracy of RSO detections. To obtain a precision ephemeris for IRAS, it was necessary to collect metric measurements of IRAS throughout the 10-month operational life. The archives of NAVSPASUR and the SSC[1] were utilized to obtain all of the available tracking data on IRAS throughout 1983. Precision orbits were fit to the data using 8-day arcs with 1-day overlaps. A special perturbations orbit determination routine, called DYNAMO, was used for this job with an accurate model of the gravitational and nongravitational forces acting on IRAS. Attributes of the DYNAMO orbit determination package are given in Figure 3.1.

The IRAS focal plane was cooled to 3 to 4 deg Kelvin using a liquid helium cryostat, which sublimated and vented as the operation period proceeded. This produced a small thrust on the platform of IRAS, which had to be modeled in the orbit-fitting procedure. This was modeled as a thrust in the along-track direction whose value was constant and estimated as a free parameter for each day of the weekly fit. To avoid correlation between the estimation of the along-track thrust effect and scales for the effect of atmospheric drag and the effect of solar radiation pressure, the area-to-mass ratio and scales were held fixed and constant throughout. Earthshine pressure was also included in the nongravitational force model for IRAS. The gravitation model included the geopotential to degree and order 20, the sun and moon, and solid Earth and ocean tides.

Table 3.1 presents the results of comparing adjacent weekly fit 1-day overlaps over the entire time period of interest, from Day 26 to 334, 1983. The average and maximum magnitude errors for the differenced position vectors are displayed for each day that an overlap test was performed. Most of the 1-day overlaps show an average magnitude error of about 60 m with a maximum of 100 m, but there are occasional instances where the average is as large as 500 to 700 m with a maximum error of close to 1 km. The data tabulated actually represent a worst case since the comparisons are made at the ends of each fit interval, which have the largest error. To show a typical weekly fit comparison result, the errors for 1-min spacing in the radial, along-track, and cross-track components for the Day 138 overlap are plotted in Figure 3.2. Note the comparison of the plots of the Day 250 overlap errors shown in Figure 3.3, which represent the worst case from Table 3.1. In Figure 3.3 large amplitudes in the 1-min sampling of the component errors are seen.

The reason for the large anomalies in Table 3.1 is not well understood, but it can be speculated that they are tied to the ability of the orbit-fitting procedure to model the thrust from the cryogen depletion. Figure 3.4 shows a plot of the daily fit along-track thrust value, which was used to model the cryogen depletion effect for IRAS. The value plotted over the 10-month life of IRAS is the thrust value in 10^{-6} dynes. Although the noise in the fit is extensive for the first week, the thrust value settles down to nearly a constant value, and the noisier aspects of the plot can be correlated to the periods in Table 3.1 with the

---

[1] We thank J. Liu and B. Morris for providing the data.

largest overlap errors. Also, the cryogenic effect on the orbit is seen dying down to nothing after the liquid helium has been entirely depleted (after Day 322). The difficulty the orbit-fitting procedure has in determining an accurate thrust value on certain days may be tied to the number and accuracy of the observed data used in the fit or else correlated nongravitational effects such as changes to the platform attitude.

The estimated error for the accuracy of the position of IRAS for an arbitrary time during the mission is 40 m, and values enlarged by an order of magnitude are likely in worst-case scenarios. As discussed in Section 2 and shown in Table 2.4, a 100-m ephemeris error during a worst-case observation scenario of 1000-km range will produce an angle error on the order of 5.7 mdeg.

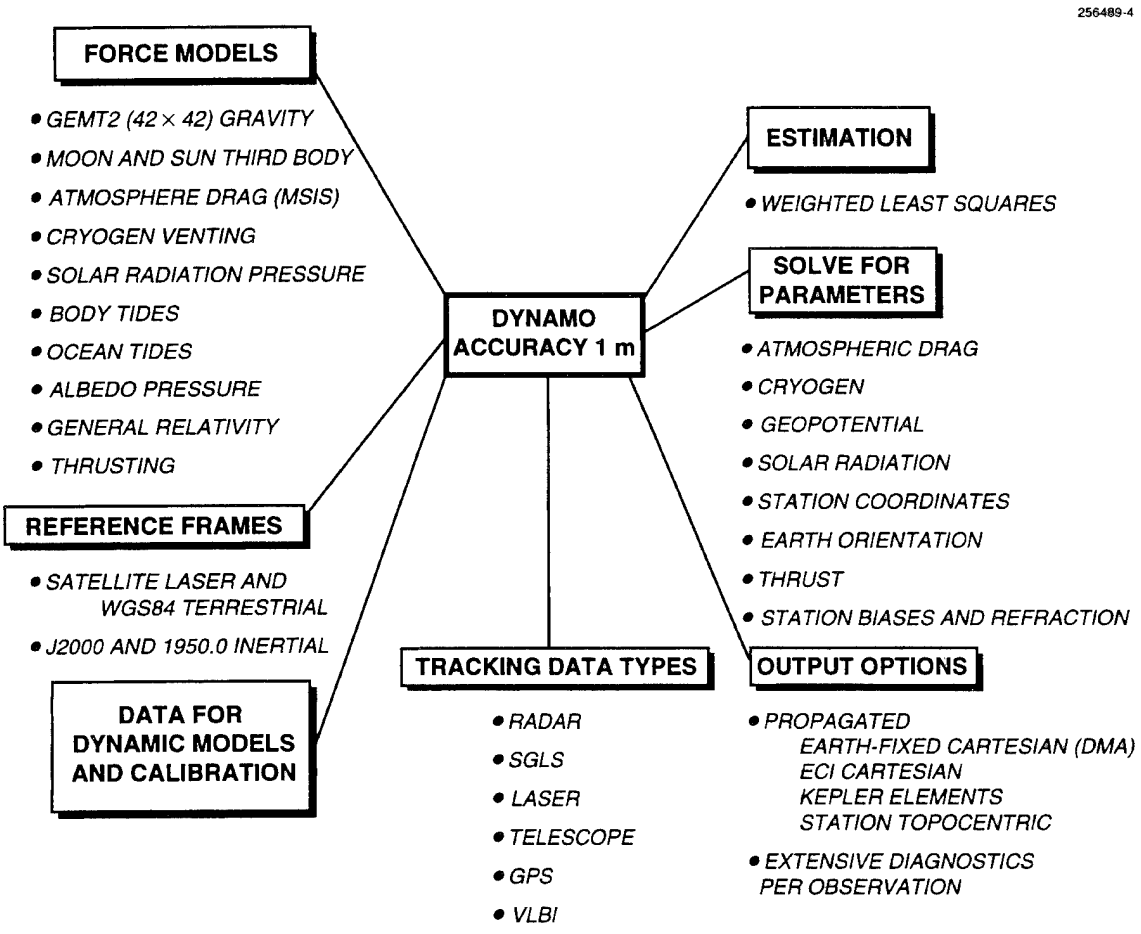

Figure 3.1. DYNAMO: A precision special-perturbations orbit determination package based on numerical integration of the equations of motion.

TABLE 3.1

Average and Maximum Magnitude Errors for Weekly IRAS Ephemeris Overlaps

Day	Ave (m)	Max (m)	Day	Ave (m)	Max (m)	Day	Ave (m)	Max (m)
033	316.8603	768.3221	138	57.5055	161.0116	243	42.1016	116.6946
040	195.5644	382.1880	145	65.1359	141.1725	250	755.8905	1221.6632
047	59.5224	99.1698	152	184.3700	607.9505	257	14.9914	24.7978
054	62.8377	160.0769	159	734.3669	968.6793	264	63.9642	195.0128
061	45.5191	103.8426	166	29.7051	89.6015	271	49.8849	105.6900
068	81.4597	192.2516	173	32.6626	87.3699	278	49.7028	126.2174
075	63.1766	98.0586	180	106.6018	204.6294	285	50.1838	137.7953
082	18.9503	48.9553	187	276.1734	426.6822	292	62.5013	168.5320
089	58.9166	122.5194	194	103.6623	344.4290	299	35.1568	83.8734
096	50.9448	127.8486	201	34.5102	66.4774	306	60.4901	123.1479
103	28.1980	55.6057	208	17.6178	44.1519	313	93.9371	264.6979
110	42.7681	82.6781	215	212.5613	852.0574	320	99.4806	239.0126
117	65.1880	167.5741	222	323.6604	483.7886	327	42.5203	94.4586
124	578.9186	785.9730	229	42.8074	93.2743	334	17.3608	41.5920
131	32.2592	57.2873	236	61.7742	134.8810			

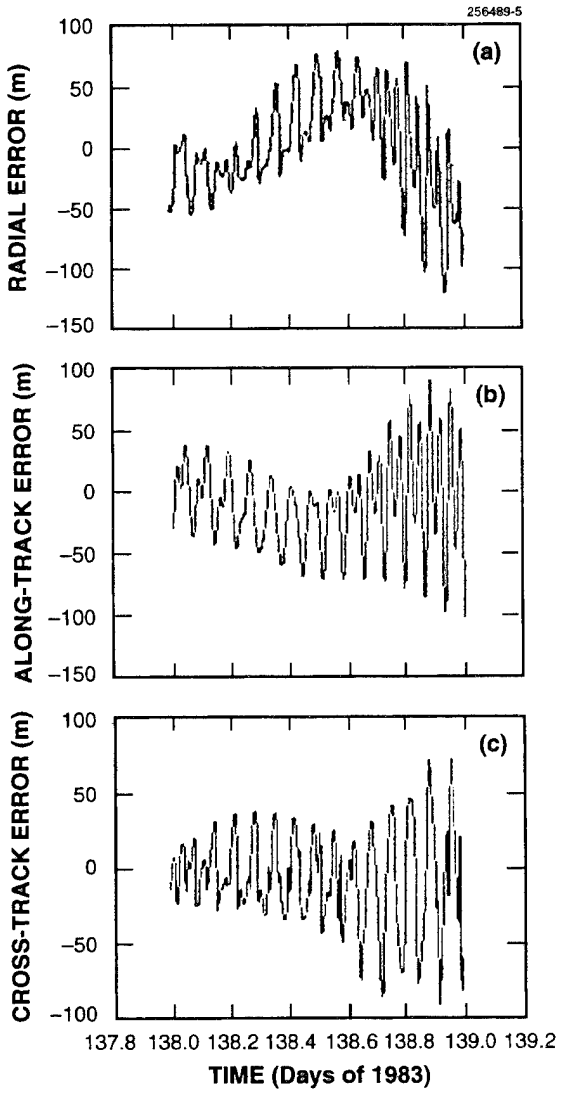

Figure 3.2. Orbit error for IRAS during the Day 138 overlap of two adjacent weekly fits (a normal sample).

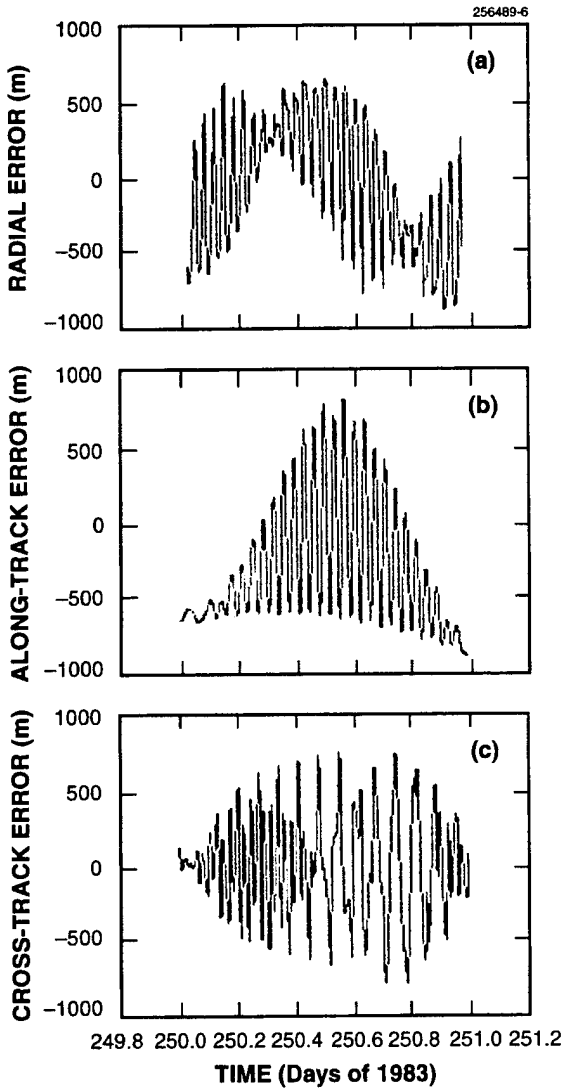

Figure 3.3. Orbit error for IRAS during the Day 250 overlap of two adjacent weekly fits (a worst-case sample).

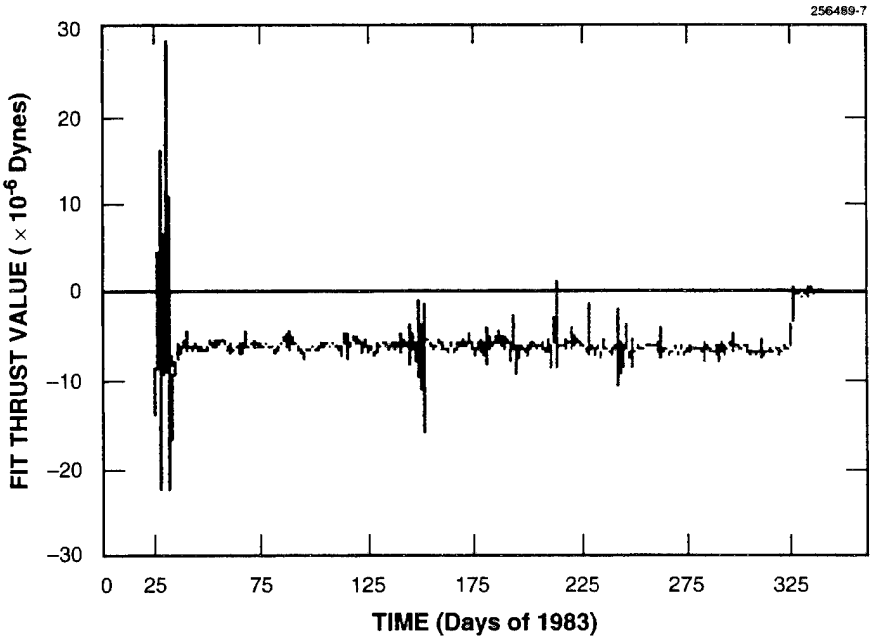

Figure 3.4. Fit along-track thrust values from the IRAS orbit-fitting procedure.

4. THE AUTOMATIC ANALYSIS DATA FLOW

The IRAS metric data were analyzed with automatic software in the MSX Surveillance Data Analysis Center (SDAC) called the Metric Pipeline. Its job is to characterize the accuracy of metric data supplied to the pipeline. It utilizes Uncorrelated Target (UCT) processing to tag the data, independent metric observations from the U.S. Air Force Space Surveillance Network (SSN), and analytic orbit determination to provide an initial orbit as a front end for follow-on precision orbit determination. Residuals of the test data from the precision orbit determination are then isolated and sent to a data base for the analyst to consider pass statistics. Figure 4.1 illustrates the data flow.

First, a UCT processor is invoked to attempt to correlate every metric observation to the known RSO catalogue, and any observation that does not correlate will be removed from additional processing. The UCT processor utilizes an algorithm referred to as "Elsets-to-Observations" correlation, which uses a series of filters with a known catalogue of RSO element sets to correlate the observations. A data flow is given in Figure 4.2. The coarse filter is used to weed out most of the element sets very quickly, and the UCT processor is able to do this by keeping all of the element sets in memory and using a quick propagator to determine rough pointing from the proper sensor for comparison with an observation at the time of interest using coarse tolerances. The few that pass the coarse filter are sent to a fine propagator to determine an RSO element set that best agrees with the observation to within fine tolerances.

What remains are sets of observations that have tags associating them with known RSOs. As shown in Figure 4.1, each set of IRAS metric observations on a particular object will follow a multistep procedure to characterize the metric accuracy of the data. All other SSN metric data on the particular RSO within, say, $\pm$ 20 revolutions of the object's orbit will be retrieved. The most recent element set on the object from the RSO catalogue data base will be retrieved. The element set will be fit to the SSN metric data using a least-squares algorithm tied to an analytic propagation model. This is done using a software package called ANODE, and its attributes are provided in Figure 4.3. ANODE is able to produce a good starting estimate for a DYNAMO orbit fit (see Figure 3.1). Pass statistics from the precision orbit of the target compared to the IRAS metric data form the basis for assessing the quality of the data.

Much of the challenge in automating the pipeline procedure is to stop, check, and restart the orbit-fitting algorithms in case of failure or nonconvergence. In some instances, ANODE and DYNAMO can fail to converge due to the presence of bad or mistagged data or because there was a maneuver during the fit interval. In cases of nonconvergence, a result produced by ANODE or DYNAMO can be worse than the catalogue initial conditions. Force modeling is determined automatically, and ANODE and DYNAMO are both asked to fit free parameters to model nongravitational effects such as atmospheric drag and solar radiation pressure. In cases of sparse data for the orbit fit, the orbit-fitting software may be unable to determine a good orbit. To restart the orbit-fitting routines effectively, ten subintervals of the basic arc of data are utilized to avoid maneuver windows or tracks of bad data. These subintervals are outlined in Table 4.1. DYNAMO is not asked to fit an orbit for an RSO for which ANODE could not converge. If the DYNAMO orbit is still unable to converge with the provided data in one of the ten intervals, then the orbit is left for an analyst to work with interactively.

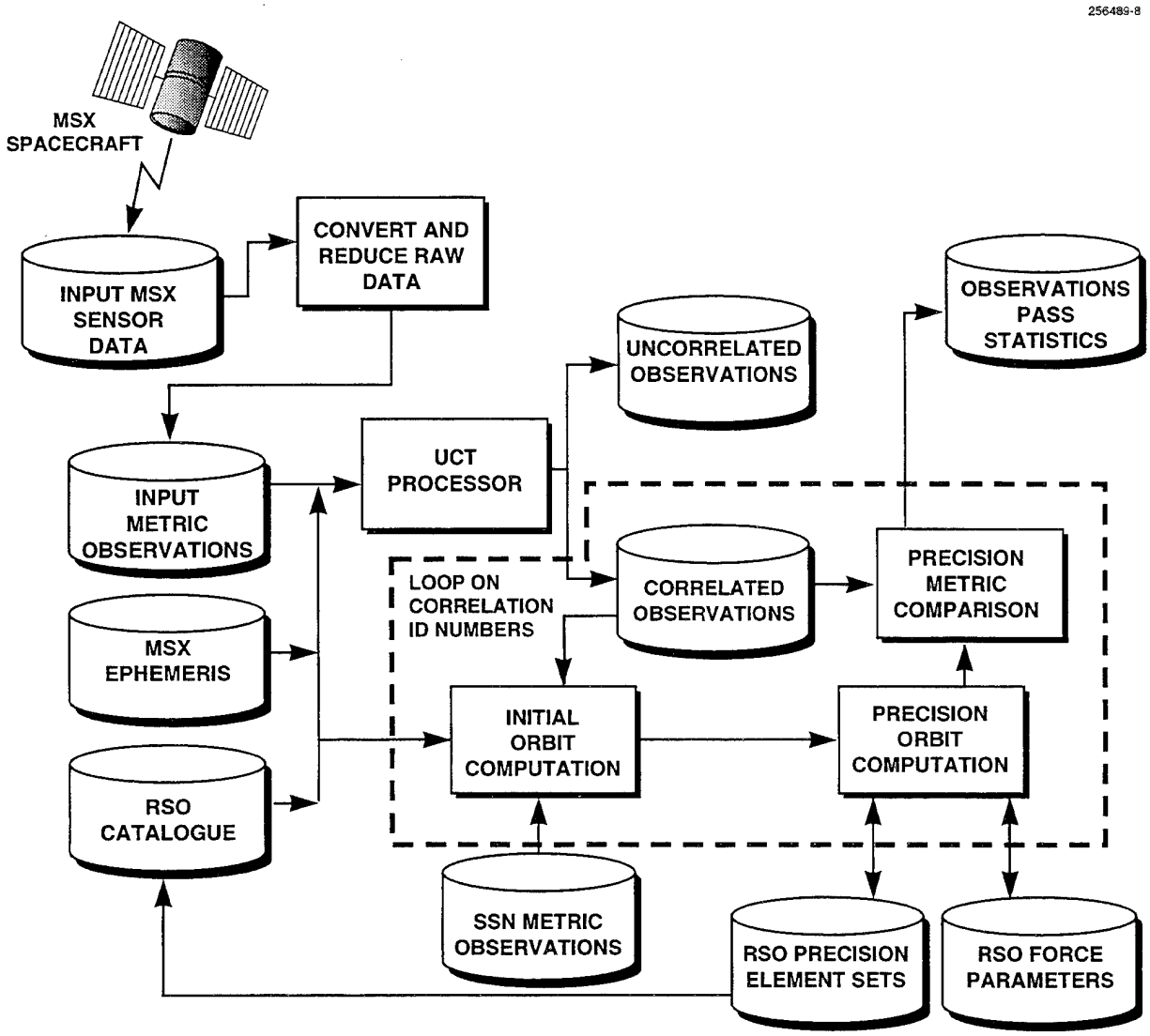

Figure 4.1. Automatic processing of metric observations in the SDAC.

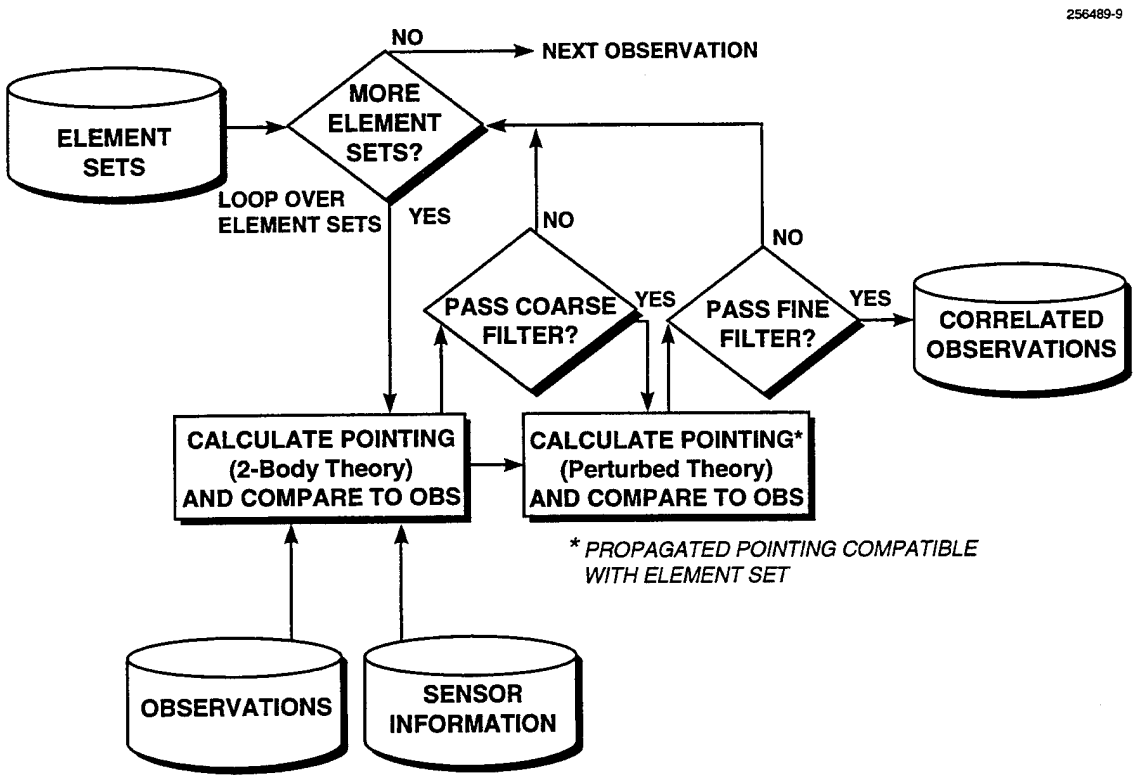

Figure 4.2. UCT processor Elsets-to-Observations correlation data flow (for use in automatic processing of metric observations in the SDAC).

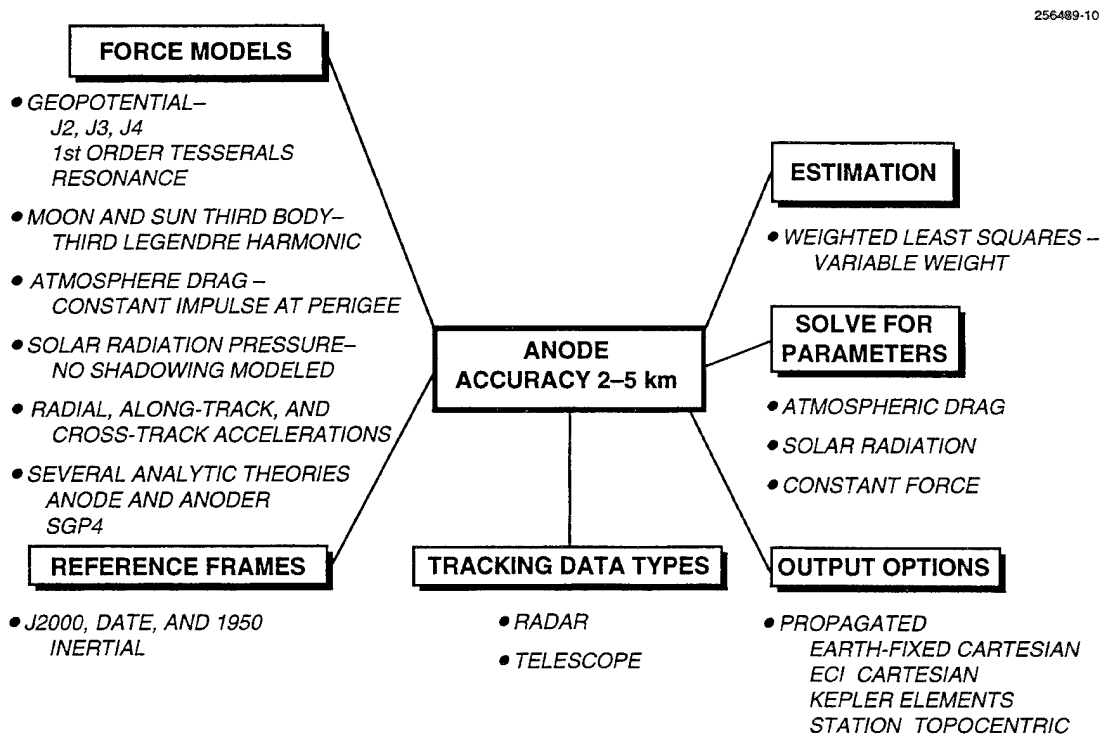

Figure 4.3. ANODE (for use in automatic processing of metric observations in the SDAC).

TABLE 4.1

Restart Schedule for ANODE and DYNAMO in the SDAC Metric Pipeline

Restart Level	Time Interval for Fit
Start	(D – 20/R, D + 20/R)
2	(D – 10/R, D + 10/R)
3	(D – 5/R, D + 5/R)
4	(D – 20/R, D + 2/R)
5	(D – 10/R, D + 2/R)
6	(D – 5/R, D + 2/R)
7	(D – 2/R, D + 20/R)
8	(D – 2/R, D + 10/R)
9	(D – 2/R, D + 5/R)
10	(D – 1/R, D + 1/R)
D = Center Time of Data to be Characterized R = Mean Motion of RSO Orbit in Revolutions per Day	

5. COROLLARY DATA TO SUPPORT THE ANALYSIS

In this section, the corollary data required to support the automatic metric pipeline will be outlined, and the source of the data in our processing will be specified. The SDAC automatic metric pipeline requires the IRAS observations in terms of right ascension and declination, a catalogue of RSO element sets for each day of the IRAS mission, and independent SSN metric observations on every object observed by IRAS.

A first pass of the UCT processor on the IRAS RSO detections was performed in late 1992 using catalogues of element sets for 1983 from the Millstone Hill radar archives [5]. However, these catalogues contain mostly deep-space satellites, and many of the satellites above the IRAS altitude and with a period < 225 min were not included. Moreover, Millstone does not routinely receive SSN metric data on these low- to midaltitude satellites. NAVSPASUR was requested to complete both the required element set data and the SSN metric data. Complete catalogues of RSO element sets for each day of 1983 (totaling over 4500 element sets per day) and archived metric data on all tracked objects for the year (totaling more than 570 Mbytes) were provided.[2]

The metric data from the NAVSPASUR archives from 1983 were not of the same quality that are available for the 1995 SSN. This fact clearly demonstrates the quality calibration work done over the past 12 years to enhance the SSN metric data and (as a by-product) the element set catalogue. The optical sensors in use during 1983 included GEODSS and the Baker-Nunn cameras. The latter produced poor quality angle data on the order of 10 to 30 mdeg, while GEODSS produced angle data with 5- to 10-mdeg accuracy, 1 sigma. Radar sites in use included the Millstone Hill radar, the ALTAIR radar, and Pirinclik, Turkey (the FPS-79). Pirinclik data were of poor quality, with range errors on the order of 60 to 100 m; Millstone data had a range quality of 5 to 10 m, with angle accuracy of 5 to 20 mdeg; and ALTAIR data were somewhat worse.

The density of the archived metric data provided by NAVSPASUR was smaller than when each object was tracked, to save on resources. To trim the amount of archived data, NAVSPASUR consolidated measurements from the tracks and made Earth-centered state vectors out of some of the tracks of observations. This has the effect of causing the precision orbit program to produce orbits of a poorer quality. Many of the orbits computed for characterizing the metric accuracy of an IRAS track are of a similar quality to the IRAS ephemeris itself, about 40 to 100 m. Thus, the reference orbits also contribute to the metric error budget as a bias in the residuals.

---

[2]The authors thank Robin Smith and the NAVSPASUR archives for providing the data.

6. RESULTS

A summary of the results from processing all of the IRAS data from the debris data base is shown in Table 6.1. The total number of RSO tracks based on a precision metric correlation, the number of days, the number of distinct satellites, the average and standard deviation of the tracks per day, and pass statistics for the tracks are tabulated. In this section, the following results are displayed: the average and standard deviation of the bias errors in both right ascension and declination for the tracks and the average and standard deviation of the standard deviations in both right ascension and declination for the tracks. All values for the statistics are given in millidegrees. As seen in Table 6.1, the average right ascension and declination bias errors are small, but there are large standard deviations for these values. Thus, the tracks sometimes exhibited very large biases (> 30 to 50 mdeg) and other times had smaller values. The average standard deviation in right ascension was about 10.9 mdeg, while the value for declination was considerably better (7.0). There is also a large value (close to 13 mdeg) in the standard deviation of these results in both right ascension and declination.

IRAS saw a wide variety of objects, including noncircular low-altitude orbits with apogees higher than the IRAS orbit. The metric error budget for IRAS data, which includes time and IRAS ephemeris errors, can be smaller for certain classes of objects. The time and errors from the IRAS ephemeris can be negligible for objects in geosynchronous orbit because the observation range exceeds 35,000 km. Unfortunately, precision reference orbits for these objects are difficult to produce because of the lack of good quality angle-tracking data from the independent SSN sensors. Accurate range data is of less value for geosynchronous orbits if the angle tracking data have a metric accuracy of 10 mdeg or more. Nevertheless, it is interesting to consider all of the IRAS tracking data on geosynchronous RSOs. The data are tabulated in Table 6.2, showing that IRAS saw a large number of geosynchronous objects with much better declination accuracy and slightly better right ascension accuracy. The nature of the bias errors do not change for this category of objects, which suggests that the pointing and reference orbit errors may be the chief contributors.

The results in Table 6.2 are not as good as one might expect, due in part to a number of tracks plagued by some of the issues outlined in Section 2.2. Table 6.3 shows two sample IRAS tracks on the geosynchronous orbit SSC #13900. The IRAS track numbers are, respectively, #547347 and #547348. Table 6.3 shows the absolute time, the residuals in right ascension and declination, the detector number (for mapping on Figure 2.1), the wavelength of the detector (in microns), the range from IRAS, and the flux (in Janskys). Recall from Section 2.2 that noise values for most of the detectors were on the order of 0.2 Jy and can be as much as 0.3 Jy. All of the flux values for Track #547347 are greater than three times the noise floor, and the standard deviation of the data in right ascension is roughly 4 mdeg and about 2 mdeg in declination. Now consider Track #547348 and notice the small 60-μ detector values (0.32, 0.14, and 0.29 Jy). These may corrupt the metric accuracy considerably by skewing the direction and the in-scan velocity and, consequently, the calibrated metric positions. However, when noticing the absolute time, the time at Detector 50 in Track #547347 and the time at Detector 50 in Track #547348 are only 0.071 sec apart. At a rate of 4.58 arcmin/s, the object would travel a distance of 0.32 arcmin, which leads one to believe that these two detections are part of the same detection and track. The same is true for Detectors 54 and 42. If we

reject Detectors 37, 14, and 9 from Track #547348 and merge data from Detectors 54, 50, and 42 into Track #547347, then this leaves Detector 29 from Track #547348, which does not fit. Its flux value is much lower than the other 12-μ values for this object, and we conclude that it is not part of the track of this RSO. Unfortunately, examples such as this are not rare in the IRAS data, and these will contribute to larger biases and standard deviations. Since most of the analysis was done automatically, there was little attempt to screen out all of the bad tracks from the overall statistics, although obvious metric outliers were removed.

TABLE 6.1
Results from All of the IRAS Tracks on Known RSOs
(Angle quantities are given in mdeg)

Total Number of Tracks	1168
Number of Days Processed	277
Number of Distinct Satellites Observed	399
Average Number of Tracks per Day	4.2
Std. Dev. of Number of Tracks per Day	2.3
Avg. Right Ascension Bias (Over # of Tracks)	−5.9
Avg. Declination Bias (Over # of Tracks)	−0.6
Std. Dev. of Right Ascension Biases (Over # of Tracks)	33.0
Std. Dev. of Declination Biases (Over # of Tracks)	27.6
Avg. Right Ascension Std. Dev. (Over # of Tracks)	10.9
Avg. Declination Std. Dev. (Over # of Tracks)	7.0
Std. Dev. of Right Ascension Std. Dev. (Over # of Tracks)	13.1
Std. Dev. of Declination Std. Dev. (Over # of Tracks)	12.2

During the course of the pipeline processing of the IRAS metric data, there were instances where ANODE indicated that the IRAS track contained good data, but the follow-on DYNAMO orbit would not converge. In these cases, the analyst is forced to interactively work with DYNAMO to produce a good reference orbit. Reasons for DYNAMO's failure to converge include bad observations in the SSN data set or data mistags, an attempt to fit nongravitational parameters that could not be supported by the data, and ANODE's failure to provide a good enough initial orbit. In other instances, correlation tolerances were passed in the UCT processor using an existing element set, but ANODE was not able to converge well enough to satisfy goodness-of-fit requirements for the automatic pipeline to proceed onto a follow-on

DYNAMO orbit. In each of these instances, the user is forced to look at the data interactively. For the IRAS data, these instances occurred between 10% and 15% of the time because the data on some satellites are sparse or noisy and some satellites performed maneuvers outside windows where they were observed. Some interactive solutions have been obtained for this study, but many remain. Therefore, the totals given in Tables 6.1 and 6.2 may not indicate all the known RSOs that IRAS observed. It is estimated that the total in Table 6.1 can be increased by about 100 or 150.

TABLE 6.2

Results from all of the IRAS Tracks on Known Geosynchronous RSOs

(Angle quantities are given in mdeg)

Total Number of Geosynchronous Tracks	137
Avg. Right Ascension Bias (Over # of Tracks)	−4.7
Avg. Declination Bias (Over # of Tracks)	−1.2
Std. Dev. of Right Ascension Biases (Over # of Tracks)	42.8
Std. Dev. of Declination Biases (Over # of Tracks)	26.4
Avg. Right Ascension Std. Dev. (Over # of Tracks)	9.5
Avg. Declination Std. Dev. (Over # of Tracks)	3.6
Std. Dev. of Right Ascension Std. Dev. (Over # of Tracks)	11.4
Std. Dev. of Declination Std. Dev. (Over # of Tracks)	7.0

TABLE 6.3

Example of Two IRAS Tracks Correlated to the Same Object Closely Spaced in Time

#	Day (1983)	$\Delta\alpha$ (mdeg)	$\Delta\delta$ (mdeg)	Det #	Bnd (μ)	Range (km)	Flux (Jy)
IRAS Track ID Number 547347 (In-Scan Velocity = 4.58 arcmin/s)							
1	91.3953633231	9.4	−8.3	54	12	34878.5	4.50
2	91.3953667841	4.4	−7.7	50	12	34877.8	1.49
3	91.3953782325	3.7	−7.8	42	25	34875.7	4.33
4	91.3953864390	3.2	−8.0	38	60	34874.2	1.72
5	91.3954006481	2.4	−8.3	30	12	34871.6	4.41
6	91.3954121979	1.7	−8.4	22	25	34869.5	4.15
7	91.3954246848	1.0	−8.7	15	60	34867.2	1.46
8	91.3954330330	9.0	−10.2	11	60	34865.7	0.84
IRAS Track ID Number 547348 (In-Scan Velocity = 4.62 arcmin/s)							
1	91.3953605921	12.8	−0.1	54	12	34879.0	4.77
2	91.3953659632	−4.6	−1.5	50	12	34878.0	1.58
3	91.3953783547	−44.7	−4.7	42	25	34875.7	4.42
4	91.3953874091	−74.0	−7.0	37	60	34874.0	0.32
5	91.3954025895	−123.1	−10.9	29	12	34871.2	1.29
6	91.3954274591	−203.6	−17.4	14	60	34866.7	0.14
7	91.3954355422	−229.7	−19.4	9	60	34865.2	0.29
Correlated Object Number: 13900							

7. SUMMARY

An automatic procedure has been used to process all potential RSO observations from IRAS. Required corollary and auxiliary data include a catalogue of RSO element sets updated for each day during IRAS operation, independent metric observations from sensors in the SSN for each object that IRAS observed, and a precision IRAS ephemeris. The latter was calculated in-house using SSN metric data on IRAS throughout 1983. A procedure of metric calibration was outlined and a metric error budget was formulated. The results illustrate the following points.

1. Although IRAS was pointing away from the Earth in a configuration conducive to astronomical observation, RSOs were seen on the average of four tracks per day. IRAS observed nearly 400 distinct RSOs with representatives from most satellite orbit classes, except those with apogee height less than the height of IRAS.

2. Even though the data base of potential detections contains nearly 139,000 tracks, an absolute metric correlation with known RSOs was made for nearly 1200 tracks (or $< 1\%$). It is speculated that there may be as much as an additional 1% of the data base that is comprised of uncorrelated satellites (debris and uncatalogued objects), but more than 97% of the data base is uncertain and many of the detections may be spurious.

3. Metric calibration of the tracks of observations is difficult because of the potential for erroneous detections corrupting the in-scan velocity and direction and, consequently, the absolute position. It is estimated that (for tracks without erroneous observations) the accuracy of the right ascension is 10 mdeg and the declination is 3 mdeg. These are comparable to GEODSS metric accuracy values for 1983.

APPENDIX A

IRAS TRACKS CORRELATED TO KNOWN RSOs IN THE CATALOGUE

This appendix lists all of the IRAS tracks correlated to known RSOs, for which a precision metric comparison to an orbit determined from independent SSN metric data was made. The following data are provided for each track: The absolute time of the first detection in the track, the correlated RSO SSC object number, the standard deviation (per unit weight) from the DYNAMO fit to independent data, and the right ascension and declination biases and standard deviations. The Sigma value indicates a goodness-of-fit criterion, and the results can be scaled by that value. If the orbit is fit to the data so that the residual errors are on the order of the weights on the data, then the Sigma value would be 1.0. If it is more, then the orbit errors are worse than the weights; if it is less, then they are better than the weights. Statistics from the IRAS data where the Sigma value is greater than 10 are suspect.

Track#	time (Days from 1983)	Object#	Sigma	ra bias	ra sd	dec bias	dec sd
1	41.6147528169	10092	1.6	-26.8	53.0	-67.7	49.9
2	41.5345997520	11054	0.9	8.5	12.4	4.6	3.2
3	41.6164950315	12959	14.9	-74.5	2.2	-106.9	2.0
4	41.4198864954	13607	1.4	-30.7	36.0	-21.7	11.2
5	41.5366308990	8838	5.9	-45.8	57.8	64.7	3.9
6	41.5366706564	9047	3.8	-20.6	9.5	26.4	17.2
7	41.4324052933	9843	0.8	-20.0	22.2	-7.5	44.4
8	41.2827374609	11728	3.0	-8.0	4.4	-9.0	1.4
9	42.1417416639	12967	3.3	11.3	8.6	-115.3	0.5
10	42.1113186022	1804	1.1	-1.1	3.3	26.6	28.4
11	42.1143300471	9049	19.7	92.0	8.8	9.0	5.3
12	43.6192506448	10455	2.5	13.0	23.5	-51.8	8.7
13	43.4900564146	11328	0.3	-4.5	22.8	-7.5	1.8
14	43.9907490229	11328	0.3	-19.8	11.9	-12.4	2.3
15	44.1215433059	10455	1.1	-8.7	6.5	-25.1	3.3
16	44.1469022455	13025	2.1	-19.5	5.3	-5.3	2.5
17	44.0631770552	7276	0.7	9.1	34.1	-7.0	6.9
18	44.1208650076	9049	19.7	68.0	2.4	10.3	0.9
19	45.9946912356	11328	0.3	12.1	4.1	-8.6	0.8
20	45.6246672147	9269	0.0	7.0	26.6	-44.4	23.5
21	45.6137524251	12851	1.1	0.7	4.2	4.0	1.3
22	46.1513847333	11621	0.3	-18.7	6.8	8.7	0.8
23	46.1051365528	11791	0.6	6.2	34.2	24.4	20.0
24	46.1512172448	12339	1.8	-11.4	2.5	3.2	0.5
25	46.0534053356	13237	1.0	-5.2	1.9	-2.2	0.9
26	46.8309395801	13753	1.0	-1.8	8.0	13.9	0.9
27	46.0657793465	8822	3.4	-6.7	10.6	-5.0	4.8
28	46.1269519838	9049	19.7	18.2	6.8	26.1	3.7
29	47.0413444869	11054	0.7	-10.0	11.5	10.3	2.1
30	47.1220108787	12561	4.7	45.3	6.7	33.0	1.7
31	47.1301747755	9049	19.7	18.7	3.5	19.9	2.0
32	47.7630287624	4712	0.6	53.8	56.0	47.0	26.3
33	47.0672454082	608	2.2	8.5	4.3	-40.2	63.2
34	48.5543194397	10669	0.6	-17.5	13.8	5.5	0.4
35	48.0005039542	11856	1.3	1.0	3.3	-5.2	0.3
36	48.5024457009	11856	1.3	4.1	8.9	-4.6	1.1
37	48.5540835918	12065	1.4	-47.7	1.9	-4.0	0.5
38	48.7761539267	12680	1.6	16.5	5.4	121.6	6.5
39	48.8367019447	10143	2.7	-1.4	16.3	3.6	1.6
40	49.0444240318	11054	0.9	-13.8	6.6	5.7	2.0
41	49.0027024186	11328	0.8	36.4	33.2	-7.5	0.3

Track#	time (Days from 1983)	Object#	Sigma	ra bias	ra sd	dec bias	dec sd
42	49.5582348706	11718	0.3	-12.7	28.7	-0.6	2.3
43	49.0751536127	7276	0.7	3.3	8.8	-8.6	0.6
44	50.3718051304	12787	6.8	-71.5	3.9	-30.9	2.8
45	50.0622140779	13237	2.2	-21.1	4.1	-3.1	3.1
46	50.5580852705	13069	6.2	-30.6	15.0	-9.9	1.0
47	51.6305244539	12561	6.0	63.5	3.2	28.3	1.6
48	51.9963727243	13237	1.7	35.3	36.2	-0.6	17.9
49	51.8386980814	13610	1.5	-5.9	2.5	20.9	1.7
50	51.6345643208	6939	1.4	7.6	1.3	30.2	0.3
51	51.0550405744	11728	3.0	-0.2	2.9	7.7	0.8
52	52.1354813311	12561	4.9	55.3	10.9	43.7	1.6
53	54.5193948525	7260	18.1	-39.5	1.8	-19.2	0.8
54	56.1021928829	13652	11.1	85.9	15.9	41.4	6.4
55	56.5687818543	13652	11.1	149.8	12.1	-39.0	2.1
56	56.5615527391	7545	3.5	-25.9	7.1	7.8	2.7
57	57.1607690869	11554	4.2	-7.9	7.6	-21.4	3.1
58	58.1761445698	12447	2.9	-28.5	6.9	-7.6	0.1
59	58.6433587398	13631	3.1	42.1	5.3	-40.3	0.9
60	59.7171315799	12561	4.9	122.9	0.8	-72.3	0.8
61	59.7717538633	12624	0.7	-4.3	0.1	24.2	1.3
62	59.9152081623	12679	1.2	-3.1	3.7	-3.5	14.1
63	59.5450004516	341	0.7	3.0	14.4	-17.8	20.0
64	59.0802435514	7376	1.3	31.1	7.6	-3.3	0.4
65	59.5076542036	8838	0.8	-8.4	3.0	-0.2	4.1
66	59.6546850990	9269	2.4	12.6	1.0	-4.8	0.7
67	59.7862465843	9330	1.7	-12.4	11.0	4.1	3.5
68	60.6060076025	10091	1.4	-9.4	16.6	-11.8	7.3
69	60.4564003622	11384	1.2	-9.8	0.5	-9.3	5.4
70	60.0036620191	11440	2.6	-121.0	1.4	40.0	0.1
71	60.5316016941	12563	3.8	-0.3	27.2	-24.4	7.2
72	60.7209470358	6691	1.8	-7.0	5.7	7.7	0.1
73	60.0839148698	7376	0.9	7.1	7.3	-12.4	0.8
74	60.1095921611	8366	2.3	-21.0	8.2	1.2	0.9
75	61.2563300030	10557	1.2	-48.6	6.1	3.0	1.3
76	61.4598911977	12920	0.4	69.7	2.9	23.6	0.3
77	61.2513907282	12933	0.8	-2.7	5.3	-2.7	3.5
78	61.5814304166	13652	3.1	-19.5	4.6	-17.0	0.9
79	61.0885219841	7376	0.9	16.3	3.6	-16.3	0.6
80	61.0197949426	8521	3.4	-128.9	2.3	-5.2	1.3
81	62.5918548455	7372	1.8	-11.6	6.8	7.7	1.5
82	62.1891187613	8910	30.4	37.7	27.8	20.2	11.8
83	63.0106489976	11440	2.6	-58.7	13.6	33.6	3.1
84	63.6078025035	13075	0.5	17.3	35.9	-6.7	16.2
85	63.5372434726	628	1.7	-46.6	8.7	15.3	34.4
86	63.6075177976	7800	1.3	4.6	2.5	-5.0	0.8
87	63.4762759694	8482	8.0	-96.1	8.5	-7.4	1.6
88	64.5380760882	7780	0.8	-17.9	6.0	-8.0	1.2
89	64.5385698494	8425	0.8	0.0	2.4	-5.0	0.1
90	64.3235493916	9911	1.0	3.8	2.3	-9.6	1.6
91	64.2635316699	10557	0.8	-17.9	5.8	-1.6	0.6
92	65.5403518428	9941	1.4	18.0	0.5	-5.7	0.0
93	65.0397520677	8425	0.5	-6.7	14.7	-5.4	32.7
94	65.5438476464	11007	1.8	-3.6	11.3	16.4	2.8
95	66.5493687823	11589	2.0	-13.0	4.2	-9.3	4.0
96	66.4691688587	12915	1.1	12.9	11.2	-6.0	0.8
97	67.8076355898	10143	5.8	75.7	0.1	25.9	0.7
98	67.1958467067	7586	0.8	-21.7	11.5	-4.2	1.2
99	67.1892389374	9850	0.5	-11.5	20.6	-6.4	3.3
100	67.5443432759	7260	7.4	-16.9	14.3	5.8	0.9
101	68.5288397440	10669	1.7	-1.6	2.0	0.0	0.2
102	68.1256206541	5975	4.5	-41.4	1.5	-37.3	0.5
103	68.0450866956	7260	1.3	7.8	4.8	72.9	7.1
104	68.6067929965	7480	6.5	51.8	18.1	18.5	4.0

Track#	time (Days from 1983)	Object#	Sigma	ra bias	ra sd	dec bias	dec sd
105	68.6067918038	7540	0.7	-14.1	19.5	18.8	31.8
106	68.8140096813	13603	4.2	-25.8	19.7	-9.2	2.6
107	69.0363185712	10803	1.4	24.2	29.6	9.0	17.3
108	69.5309465302	12065	5.9	-17.3	6.3	-3.6	0.5
109	69.1082666471	7480	10.4	76.2	7.0	-3.7	0.9
110	69.1085880649	8600	1.0	11.6	12.1	-3.3	1.5
111	69.0541170617	10605	2.9	-36.8	44.0	93.0	19.3
112	69.5555693810	10605	2.9	-69.4	4.0	104.4	3.2
113	69.0802864634	12679	1.2	2.3	4.3	9.3	7.0
114	69.1082666471	7480	16.1	44.2	7.0	10.5	0.9
115	69.9651289807	11888	2.7	6.0	14.7	0.3	1.9
116	69.1920886355	13124	7.5	-0.5	1.6	-7.2	0.1
117	70.5332851855	12065	5.5	-9.7	18.2	-13.7	1.2
118	70.0273718025	12368	1.2	-9.2	2.6	2.8	2.4
119	70.9686690499	12384	4.1	14.4	6.6	-8.7	9.2
120	70.5996440324	13269	3.4	14.2	12.8	-2.7	0.6
121	70.8731258149	3174	1.3	-5.0	19.6	33.8	0.8
122	70.5546811964	7583	1.1	42.1	3.9	-17.2	0.2
123	71.2014126134	10722	1.4	-10.2	2.9	-3.2	0.4
124	71.4800452343	11861	2.4	26.9	1.3	-5.2	1.9
125	71.8867944675	11941	2.1	8.6	1.9	13.4	1.0
126	71.5355553377	12065	5.5	-6.2	5.2	-14.1	0.4
127	71.5667273839	13107	0.9	-53.4	7.8	-87.4	0.7
128	71.0972816231	7545	3.2	1.5	3.0	50.2	9.2
129	71.1032284480	9411	1.8	2.4	17.5	7.4	7.1
130	71.0621289589	11684	1.8	-35.6	15.6	-3.2	1.3
131	72.4976808558	1361	1.1	-101.7	73.7	40.2	73.9
132	72.0171764022	3177	0.5	-3.1	1.9	6.9	0.6
133	72.4846865653	7260	1.2	9.4	6.4	-3.2	0.9
134	72.4833492992	11328	2.6	-4.9	2.7	-10.2	0.7
135	72.9602731646	8482	2.3	-3.5	7.0	2.0	0.7
136	73.5401519590	12065	5.6	25.7	12.7	-13.0	0.5
137	73.4140976778	13875	1.0	4.2	23.3	0.3	10.5
138	73.1291626789	746	1.4	21.3	41.6	20.3	9.3
139	73.5582037860	7276	0.5	2.2	8.4	-23.6	0.7
140	73.2170664753	13606	3.7	-9.5	8.7	1.9	0.4
141	74.7503592909	10778	2.3	19.2	0.2	10.4	0.4
142	75.7527925822	10778	2.3	-34.8	3.1	7.8	0.5
143	75.6095846999	12339	1.4	-19.7	5.3	-3.4	3.5
144	75.1091266691	9330	0.5	22.0	7.1	-8.9	4.2
145	75.0632614289	7276	0.5	7.5	9.2	-22.2	0.2
146	76.8944522471	10025	1.0	-20.6	5.8	-0.5	0.4
147	76.7550646002	10778	1.3	-44.0	8.7	8.5	0.6
148	76.6835097417	11728	3.5	71.7	17.3	-3.6	1.5
149	76.6118199262	12339	1.4	1.6	4.7	-3.5	0.1
150	76.1129976971	13112	0.8	-8.6	27.0	20.0	10.9
151	76.9963765838	13882	1.4	-6.6	7.2	2.5	4.9
152	76.5806278759	515	1.1	-7.1	3.7	22.4	4.5
153	76.3592907863	8751	2.4	-10.6	5.5	-7.0	0.8
154	76.6079505686	13909	6.7	43.3	53.4	-54.0	34.6
155	77.5759030405	10722	1.5	-26.5	9.9	-1.6	0.2
156	77.7574678927	10778	3.2	-14.2	6.7	10.9	0.4
157	77.5084259618	11440	2.5	27.3	16.3	5.3	0.1
158	77.4992495144	12066	1.3	-9.5	9.0	-12.8	0.6
159	77.8286257674	12906	0.5	-15.2	13.5	-8.3	0.3
160	77.0621429573	2255	2.1	-22.7	7.9	14.3	5.8
161	77.6755345117	3557	0.5	18.0	24.6	8.9	187.7
162	77.4267569181	8015	0.7	-18.1	4.1	-30.1	0.3
163	78.6795895909	10893	0.4	12.7	15.6	14.6	1.1
164	78.0004617795	12066	1.4	-106.3	156.5	-2.1	58.7
165	79.7624356481	10778	3.0	-24.5	3.5	11.8	0.9
166	79.0542117559	11553	0.8	-10.4	3.8	4.3	0.6
167	79.5606274010	11553	0.8	5.6	6.4	4.0	1.1

Track#	time (Days from 1983)	Object#	Sigma	ra bias	ra sd	dec bias	dec sd
168	79.5623244503	12827	0.9	-29.0	8.1	-10.5	4.3
169	80.9909298563	12156	1.5	-3.5	7.2	3.8	0.8
170	81.5637156567	10155	0.9	-18.3	5.3	4.6	1.0
171	81.6354914566	11550	0.8	3.1	4.4	7.5	0.5
172	81.6356422655	6939	1.7	-8.1	9.6	4.5	1.5
173	81.6252138042	8476	1.3	-35.4	55.1	6.4	41.9
174	81.1302451507	8621	1.4	0.9	1.7	2.6	0.9
175	81.9944681047	9269	3.1	4.5	14.6	14.8	1.8
176	82.8521947139	12827	1.5	-44.1	3.4	-8.5	0.7
177	82.6280557619	8476	0.6	-25.4	5.9	1.2	0.6
178	83.7728624738	10778	2.7	-47.9	0.3	11.0	0.2
179	83.9955065775	13237	1.2	-44.8	48.5	4.5	0.9
180	83.2283979846	8418	0.9	-13.7	16.0	-8.6	0.8
181	83.6300096425	8476	0.6	-29.6	19.0	1.0	1.2
182	83.5501151223	9911	1.1	14.1	58.2	9.4	37.3
183	83.3114406759	9933	10.9	9.1	14.0	19.1	5.4
184	84.6309536512	12339	1.8	-21.9	4.6	0.8	0.4
185	84.2330551619	13124	0.1	-10.5	12.6	3.2	3.6
186	84.0977936302	503	1.1	-41.8	20.4	3.1	13.5
187	84.5855275897	7276	0.5	8.8	4.1	-23.3	1.4
188	85.6881922638	12679	1.0	4.4	5.2	6.2	6.8
189	85.0241231630	8838	1.4	-22.6	8.1	14.4	1.5
190	85.0237041707	8918	1.6	-38.1	2.4	-2.9	0.3
191	85.0240992590	9047	1.9	-47.0	3.9	9.3	0.7
192	86.8488672838	7324	3.1	42.9	79.9	12.5	33.3
193	86.2282881698	9927	1.1	3.1	6.7	-6.0	1.4
194	87.0953195155	10722	1.6	-14.0	3.3	-4.3	0.2
195	87.1599005369	12833	1.0	56.7	3.0	-42.1	0.6
196	87.0909351068	7276	1.1	11.5	7.1	-3.6	1.3
197	88.4595059639	13554	3.5	265.0	2.0	-21.6	0.3
198	88.5931186615	7583	0.7	2.5	3.9	3.3	2.2
199	88.5225012566	8195	5.6	20.4	7.1	-39.6	0.4
200	89.5020879913	10167	1.2	5.2	3.0	2.2	0.3
201	89.4613961728	11567	2.0	11.0	5.9	-1.9	1.1
202	89.9632479681	13035	7.3	43.8	6.2	-55.4	1.2
203	89.5050256282	13069	3.4	12.4	5.1	-8.4	0.7
204	89.0942559873	7583	5.6	6.7	6.5	-27.9	0.3
205	89.0239071082	8195	0.6	7.1	6.9	-2.0	0.1
206	89.5221591924	9941	0.7	-2.8	3.9	-1.6	0.3
207	90.0254659331	11075	1.7	-38.9	2.7	-58.8	0.8
208	90.1671815389	13205	0.5	12.1	23.5	-12.0	22.8
209	90.3818109178	6877	1.0	-1.1	0.6	-9.5	0.2
210	90.3821009256	7373	0.5	-22.4	23.4	17.9	7.3
211	90.5246894700	9829	6.1	38.8	16.0	41.7	5.2
212	90.0232452992	9941	5.4	-160.3	5.0	17.1	3.5
213	91.0368522418	11571	1.8	-24.4	5.9	-1.4	0.5
214	91.4555335978	12556	1.3	-6.1	6.5	-5.0	0.5
215	91.0976518444	12833	1.0	8.9	2.7	-1.1	0.1
216	91.3953633231	13900	3.7	4.3	3.2	-8.4	0.8
217	91.3953605921	13900	3.7	-46.7	54.5	-4.8	4.3
218	91.9252288765	2520	2.6	-0.2	10.3	118.1	1.7
219	91.0254935650	9829	6.1	28.1	19.3	13.1	59.2
220	91.3950267837	8482	5.0	-18.5	3.1	-1.3	0.1
221	92.1111948602	11570	2.7	-8.0	8.9	-4.0	1.0
222	92.0329592043	11662	1.1	-7.3	11.3	9.0	0.6
223	92.5344440123	11662	1.1	-7.6	15.2	7.8	1.2
224	93.0426056176	10061	3.0	-17.2	2.2	-1.7	1.8
225	93.0317212355	11007	6.5	-102.4	6.5	-99.6	0.5
226	93.0320145646	13215	2.2	-0.7	3.4	-7.0	1.2
227	93.0423500928	8585	4.2	-24.2	0.3	5.8	0.2
228	94.0449085894	10061	3.0	-15.0	3.2	-0.6	1.8
229	94.1172652353	12339	1.7	-13.6	6.0	34.0	1.1
230	95.5387089869	13890	1.7	10.7	7.2	-5.1	1.6

Track#	time (Days from 1983)	Object#	Sigma	ra bias	ra sd	dec bias	dec sd
231	95.2541820660	8018	1.7	-34.4	30.8	-5.4	21.9
232	96.5432220275	11662	3.2	10.8	6.2	34.4	1.2
233	96.8559463745	12624	1.3	16.4	15.3	-8.8	1.6
234	96.4047780988	12810	1.2	-1.5	11.0	-1.7	1.7
235	96.0398176324	13890	1.7	-2.4	14.3	1.5	4.7
236	96.4689379741	6877	1.6	-30.7	7.7	-19.5	2.3
237	97.5222891584	11240	1.5	-16.8	5.1	-1.0	4.1
238	97.0441960610	11662	3.3	9.9	4.3	24.7	0.5
239	97.0438996521	7373	1.6	-8.8	14.4	1.6	2.2
240	97.5248289637	8621	1.8	-1.8	6.9	1.3	1.6
241	97.5887943101	11256	6.2	-134.1	19.1	-17.9	4.3
242	98.6262525247	10002	1.5	-22.8	6.5	4.9	0.8
243	98.0542716767	10061	2.0	-10.6	1.3	-3.4	2.7
244	98.1262470524	12339	6.2	42.9	6.8	-8.7	1.6
245	98.8769006509	8482	5.0	-9.2	41.2	-11.9	37.1
246	98.2569711962	12032	1.4	4.5	2.7	-7.9	1.8
247	99.2583824370	11075	1.7	107.0	6.4	25.5	2.9
248	99.4124650942	11567	2.0	-5.5	8.9	-1.0	1.5
249	99.2581193123	12032	0.6	-7.6	3.1	-3.0	1.5
250	99.5936404522	12309	7.3	-43.5	6.5	-24.6	3.3
251	99.5448318847	7586	7.0	68.3	3.8	21.4	1.4
252	100.0473101405	11856	13.5	-117.8	3.0	-37.1	2.1
253	100.5964267983	12309	7.3	-21.5	0.6	-21.2	0.3
254	100.4106319983	12810	0.6	7.4	16.5	0.6	15.7
255	100.0475770675	13070	1.1	-5.1	4.4	-1.7	3.8
256	100.7406766060	8621	1.7	-16.0	7.1	0.2	0.7
257	100.4062434619	8701	1.1	-23.2	15.6	4.1	9.2
258	101.8848392812	11567	2.3	-14.7	6.9	0.4	0.4
259	101.5991650279	12309	7.3	-16.3	6.7	-21.6	2.0
260	101.8249246137	12311	1.6	4.6	5.9	12.4	2.9
261	101.5492492650	12368	0.9	-12.3	8.7	6.3	4.5
262	101.6095968968	13090	1.9	7.4	7.7	4.2	0.5
263	101.5510971745	13882	1.6	1.3	4.6	2.3	4.0
264	102.8245923916	11550	2.5	-25.4	13.1	2.6	2.0
265	102.0398903139	12303	1.7	-2.7	3.9	1.6	2.0
266	102.0501046007	12368	1.1	12.0	4.8	-9.2	5.1
267	102.8917425707	12818	1.6	-27.0	7.7	-8.9	4.2
268	102.1107857225	13090	1.4	-5.5	3.0	0.4	2.5
269	102.0367978432	8187	4.9	-29.2	2.7	-0.8	0.7
270	103.6036291572	12309	7.0	2.6	7.5	-18.8	1.1
271	103.8175510725	12447	3.0	-13.4	8.9	6.5	2.5
272	103.1057504957	12834	0.9	-34.5	18.3	-11.1	5.8
273	103.1998065096	9411	0.8	52.1	59.8	-14.2	16.8
274	103.5537580005	9927	2.5	0.3	10.7	-4.3	3.1
275	104.8867083718	10025	2.0	-7.3	7.2	-7.6	1.1
276	104.5733704235	11142	1.1	-20.7	13.7	0.0	2.0
277	104.6096687075	11509	1.8	-20.2	5.5	1.7	1.3
278	104.0605339383	7276	1.2	-8.8	8.2	36.6	2.2
279	104.5621110444	7276	1.2	-23.0	8.8	41.4	2.2
280	105.7430469912	10801	0.7	-15.7	9.4	-3.4	2.3
281	105.1361333791	12295	3.6	3.4	5.4	6.0	2.1
282	105.3410716944	2256	2.2	12.8	9.2	61.2	8.1
283	105.3511704638	4789	1.0	-18.3	0.8	12.9	24.3
284	105.0677190845	4882	5.2	-8.8	0.4	3.0	0.2
285	106.2863603529	13954	1.1	-12.8	2.0	-5.4	1.4
286	106.5662509918	7000	2.0	-2.8	13.3	-19.4	2.3
287	106.5611792274	9941	0.8	66.5	20.9	177.2	4.0
288	107.5736033961	10779	1.5	-16.3	5.9	1.9	2.0
289	107.0024308159	13651	1.4	-6.8	4.4	5.1	1.4
290	107.2841000059	13908	1.3	-8.9	4.8	-0.1	1.1
291	107.0672813127	7000	2.0	0.0	11.3	-24.2	2.6
292	107.5642831760	9829	2.1	15.0	13.9	-18.9	7.1
293	107.0623888215	9941	0.8	47.7	18.6	74.0	5.7

Track#	time (Days from 1983)	Object#	Sigma	ra bias	ra sd	dec bias	dec sd
294	107.5039906853	11570	228.9	-5.1	14.3	8.6	3.8
295	108.5725097656	6958	2.9	5.8	31.6	16.5	8.7
296	108.1400434257	8701	1.3	-11.2	14.5	2.6	3.1
297	108.0654405744	9829	2.4	34.4	6.1	-24.8	1.8
298	112.9160828120	11550	1.9	-12.2	0.9	2.3	0.6
299	112.1524286037	11758	0.9	-14.8	19.3	8.3	5.7
300	112.0133433038	13069	7.2	-25.8	6.6	-11.3	2.1
301	112.5760778611	13591	0.8	3.4	21.8	5.9	17.6
302	112.0836245612	4789	0.9	-25.2	10.6	6.0	8.7
303	112.5797046972	6958	1.6	10.8	3.7	-22.9	0.8
304	113.0811536156	10155	1.5	4.8	4.9	-16.4	0.9
305	113.2212685037	11847	2.6	17.8	3.2	-11.3	2.2
306	113.0162490720	13069	7.2	-20.8	5.2	-13.0	0.9
307	113.5814711883	13075	0.1	-2.2	2.2	-3.8	0.6
308	113.6205253382	1480	0.9	26.5	77.3	71.7	42.1
309	113.5787719904	9941	1.7	-39.9	28.2	1.0	19.3
310	114.7707540744	11569	5.0	-45.7	0.8	2.1	0.3
311	114.4477577787	11888	1.2	-22.8	17.6	7.7	1.5
312	114.8428763866	12447	1.0	-9.1	1.6	0.3	0.4
313	114.0197002718	13069	7.2	-19.2	5.3	-12.9	1.7
314	114.5913976716	5204	1.3	29.4	19.1	8.1	6.7
315	114.5608392931	7790	1.8	-8.1	0.7	18.8	1.9
316	114.5443893221	8822	2.6	15.9	8.8	28.4	8.6
317	115.5825558802	11007	2.1	-9.5	1.5	4.6	1.4
318	115.5629241269	7790	1.8	-6.3	16.7	19.5	6.7
319	115.9972645834	9574	2.2	10.6	1.9	-30.3	1.1
320	115.0824973438	9829	2.4	1.4	10.6	-11.9	6.2
321	116.5839997743	10089	0.8	5.1	1.9	-10.0	1.2
322	116.0836519551	11007	0.9	-0.9	16.0	-10.8	10.3
323	116.5852544632	11240	1.4	2.0	7.5	-4.2	4.6
324	116.5833815873	11662	1.1	-13.2	8.3	8.3	5.9
325	116.5126697863	12556	1.4	11.4	35.3	-11.0	16.3
326	116.7000906780	12834	3.2	-7.9	14.3	-18.8	3.4
327	116.0243857617	13069	7.2	-11.8	5.0	-17.2	0.6
328	116.1562279771	7000	2.2	1.7	5.3	-18.6	2.4
329	116.1645840521	8751	0.8	71.3	8.7	-25.6	2.9
330	116.0126617755	8820	0.4	-7.4	8.0	1.8	10.1
331	117.0861523975	11240	1.3	13.5	16.5	-10.6	7.4
332	117.4549184963	11926	2.4	-4.8	4.9	15.7	1.2
333	117.0615453014	12851	1.3	-6.0	5.0	-3.2	1.5
334	117.5148326440	13591	0.8	-9.8	16.0	6.2	33.1
335	117.5853736144	13890	1.3	-6.9	16.9	0.1	10.5
336	117.3825738448	4882	7.5	-0.7	4.4	2.8	1.1
337	117.0843552397	11662	134.0	-5.3	5.0	-2.0	2.7
338	118.3109294316	10722	1.3	-17.1	13.3	7.7	3.6
339	118.4523512322	10779	1.6	-10.1	7.3	0.0	2.8
340	118.6346330537	11964	2.5	-9.7	8.7	3.7	2.3
341	118.7778417551	12046	3.9	30.9	39.0	6.9	4.4
342	118.5070567675	12311	6.4	3.6	23.6	7.5	6.8
343	118.5048065288	9574	2.1	44.3	21.8	-100.8	5.6
344	119.6244751119	10893	2.7	-9.4	4.6	-2.7	4.3
345	119.6358011927	11550	1.3	-13.5	3.4	-6.2	0.1
346	119.3173147591	12070	2.1	-22.0	1.0	4.9	7.8
347	119.8515557000	7902	1.6	-20.8	10.8	9.1	3.2
348	120.3801729189	13882	0.5	21.1	10.5	-11.5	3.9
349	120.5940835480	7000	4.8	59.3	12.9	51.4	7.1
350	121.4555171922	11555	9.7	85.6	12.9	-158.4	2.4
351	121.5337201492	4925	1.2	2.7	7.0	-7.9	1.6
352	121.3188833704	8482	3.0	9.1	2.5	1.7	0.5
353	121.2184552243	4881	0.9	-53.9	11.6	44.1	3.7
354	122.3136729580	12920	0.8	3.0	4.7	-8.8	0.5
355	122.1781073185	7324	3.6	6.7	1.8	-4.0	0.4
356	124.1721496020	10167	0.9	35.1	47.1	-18.3	39.2

Track#	time (Days from 1983)	Object#	Sigma	ra bias	ra sd	dec bias	dec sd
357	124.0307189970	11553	1.4	2.6	10.0	-2.4	3.1
358	125.1138817163	11862	1.1	-8.3	9.7	5.8	2.8
359	125.2513562663	13205	0.3	-5.4	5.2	0.4	0.7
360	126.9707076439	13215	0.8	-9.2	6.2	-1.9	2.5
361	126.6514608385	7324	4.4	4.6	25.6	3.5	10.0
362	127.4741178697	10779	2.1	-66.3	26.1	12.7	6.2
363	127.4778740531	12851	1.9	11.9	5.7	1.3	2.5
364	127.5435098494	12915	2.0	-11.0	11.6	4.1	4.7
365	127.3346954738	13899	4.3	-8.0	8.0	-6.2	4.6
366	127.5526241301	4069	4.7	-24.7	0.3	15.1	2.0
367	128.1936715171	11028	1.0	51.0	87.7	-34.9	42.8
368	128.4846745021	11328	1.8	1.5	27.8	-74.2	4.1
369	128.1953978086	11862	1.3	-11.5	10.4	5.0	3.9
370	128.3338106264	12787	2.5	13.4	5.4	-20.7	4.0
371	128.4110370822	13608	0.9	-12.5	6.4	24.0	2.5
372	128.3372452191	4925	1.3	-37.5	20.8	10.4	11.5
373	128.0407709159	7372	1.8	4.3	3.9	-0.9	1.0
374	128.0109801334	10894	0.5	-9.8	9.2	-12.1	3.0
375	129.6128098958	10455	4.8	-97.0	4.5	-44.3	2.5
376	129.6118059972	11240	1.4	0.3	1.4	-0.2	1.0
377	129.0492838762	11555	3.3	-75.5	18.1	112.5	5.4
378	129.0476692949	12915	1.9	-9.7	7.3	3.4	1.8
379	129.0407563265	13107	2.5	-115.0	7.4	127.2	6.7
380	129.8012716619	8482	3.9	16.5	6.0	5.3	1.8
381	129.5486320795	9931	2.8	-13.4	5.9	-11.9	2.0
382	130.1143614231	10455	5.9	11.7	40.6	-0.2	68.0
383	130.6675643006	11076	1.4	54.9	11.7	-129.3	7.4
384	130.6144294316	12035	5.5	-22.7	25.0	-24.1	14.3
385	130.4794708199	12363	1.2	4.7	9.0	1.5	3.7
386	130.0493772237	12915	2.1	-7.7	1.3	-0.7	0.2
387	130.5610364007	4298	1.5	48.4	8.9	-21.0	5.4
388	130.5437362294	7178	1.1	-5.4	14.7	-0.2	9.8
389	130.6194860058	8762	4.8	57.7	7.2	54.8	3.6
390	131.8156440713	11556	0.4	-10.2	9.8	-0.3	6.1
391	131.6148517419	11662	166.9	13.8	3.5	-8.1	4.0
392	131.0508196256	12915	2.2	-5.2	6.7	-0.5	2.9
393	131.6171254185	13897	1.6	12.5	6.0	-16.8	4.4
394	131.8076487372	13970	2.2	-9.2	12.1	-3.5	4.6
395	132.3340623477	10059	0.3	-5.0	10.7	3.9	7.4
396	132.5280702797	11474	1.4	-16.0	11.9	-13.9	14.6
397	132.1162571021	11662	166.9	-6.1	3.4	16.0	7.8
398	132.1289583336	12339	1.2	10.1	4.4	-16.0	1.5
399	132.1214033929	7480	2.2	0.5	11.9	16.4	5.3
400	132.2595952502	8187	2.9	-23.2	7.0	-74.9	8.1
401	133.0258172650	11474	1.4	-23.1	38.1	-8.6	7.9
402	133.6310603759	11571	0.5	32.9	9.8	14.4	3.8
403	133.9660921356	11589	1.1	-12.3	3.7	-2.6	2.9
404	133.1920203222	8762	5.6	25.6	19.0	33.1	14.9
405	134.8150598848	10002	1.2	-28.0	2.0	-10.8	2.2
406	134.5885376392	10893	3.5	-10.0	33.5	-24.5	23.9
407	134.8258596269	10949	1.4	-27.0	9.3	-13.0	5.7
408	134.8177841343	12311	1.4	-22.4	12.4	-24.7	5.4
409	134.0582278957	13070	2.3	-38.7	21.5	5.4	14.0
410	134.8125330580	13658	0.4	-63.8	3.3	-27.6	2.7
411	134.9712030578	7376	1.4	-14.9	4.2	-9.9	3.8
412	134.5337123726	13431	12.9	38.7	0.4	2.2	0.2
413	135.4977417117	11556	0.4	-5.6	18.0	-1.7	11.4
414	135.6007068285	13666	1.0	-106.6	7.4	-37.3	1.6
415	135.5545509855	13890	1.6	49.1	54.6	-32.3	36.6
416	135.9723200089	7352	1.7	0.2	0.3	-12.7	0.7
417	135.9737364719	7376	3.7	80.4	9.7	24.9	8.5
418	135.0433800528	8600	0.8	25.0	53.4	9.9	87.5
419	136.4919891247	10779	5.0	27.8	6.8	-9.8	2.4

Track#	time (Days from 1983)	Object#	Sigma	ra bias	ra sd	dec bias	dec sd
420	136.9709822420	12959	1.4	-31.9	60.9	-10.6	23.9
421	136.0556872722	13890	162.5	43.1	8.1	-6.9	4.1
422	136.0439859896	6192	1.1	-14.6	6.6	-18.1	4.1
423	136.5630309845	7480	1.8	30.1	8.1	60.2	1.7
424	136.0644547529	9933	12.8	-25.1	9.5	11.5	0.1
425	137.3428947442	10155	2.3	-13.1	14.9	5.7	14.8
426	137.0259786671	11705	0.7	-0.8	28.9	9.6	21.7
427	137.2025048633	13591	2.2	-4.0	20.6	-5.6	9.2
428	137.4140603407	9411	1.4	6.9	21.6	-16.1	16.6
429	137.2024755345	13585	1.1	5.0	8.0	-3.8	3.4
430	140.8244275889	13090	2.7	56.4	4.9	-95.0	2.5
431	141.2822036269	10059	0.3	0.2	6.3	-1.2	3.1
432	141.0052498255	10669	0.8	-22.1	13.1	6.3	3.9
433	141.3513143973	10998	1.3	31.3	5.6	4.2	3.5
434	141.8974926683	11015	0.8	-5.6	20.7	-67.8	5.5
435	141.1015417696	11142	1.1	64.7	3.3	-50.6	10.2
436	141.5298367095	12679	1.3	-21.3	15.0	-19.6	7.3
437	141.7615857436	12984	1.0	-5.9	10.3	-16.4	4.8
438	141.5472661397	7250	0.9	-6.6	20.3	-5.7	8.2
439	141.1393280109	7641	6.1	6.5	3.6	14.9	1.3
440	141.1478187199	7653	1.6	1.5	1.3	10.0	0.1
441	141.3670918397	9329	2.3	-16.7	22.7	-32.0	13.5
442	141.6890653795	2253	3.8	-37.2	2.8	69.1	3.3
443	142.0673305640	11662	0.5	5.4	16.3	8.7	24.6
444	142.0075942264	12065	4.1	-36.7	4.8	31.2	2.1
445	142.8318072642	12984	0.9	-8.9	6.9	-39.3	1.8
446	142.6169593963	7354	1.0	-32.9	18.1	32.4	6.5
447	142.5888801584	748	1.1	9.2	13.7	6.9	5.6
448	142.1388625977	8741	1.4	9.5	4.5	-1.6	4.9
449	143.5759936971	11474	1.6	2.2	12.1	7.7	4.5
450	143.5731766479	13890	1.4	-2.1	3.2	-3.3	2.2
451	143.4274362375	7372	6.8	8.9	3.2	6.4	1.8
452	143.2200238315	7653	0.6	-6.3	5.4	2.3	1.2
453	143.3664101400	9579	1.2	3.3	8.3	4.9	2.5
454	144.0768203444	11474	1.6	-3.2	2.5	7.6	0.7
455	144.0743695627	13890	1.4	-2.1	7.8	-6.0	4.5
456	144.9103625398	13971	1.6	-6.3	14.6	-0.6	5.9
457	145.2942524373	3307	1.8	3.0	0.1	-33.6	14.3
458	145.5756272002	7741	1.2	60.5	7.6	-47.0	7.5
459	146.5561088985	11567	1.1	-4.1	10.1	-3.1	4.6
460	146.0179657487	13069	3.6	-33.4	2.2	19.6	0.9
461	146.2328102576	13753	5.3	5.2	6.3	11.7	2.9
462	146.0175884097	6052	1.8	-16.0	11.7	-6.8	5.6
463	146.2211477316	7480	8.3	9.5	2.6	7.4	1.2
464	146.0821974260	8274	0.8	-5.7	0.3	6.7	0.1
465	146.1565127601	9017	1.1	19.8	23.7	-5.3	13.1
466	147.7829322736	10684	1.1	-23.9	7.1	-16.0	6.9
467	147.5722609698	12627	11.9	121.8	5.8	-16.1	7.6
468	147.0205512721	13069	3.6	-23.3	8.9	15.3	4.7
469	147.6835853360	3173	0.7	8.6	5.2	12.2	5.4
470	147.2227016144	6958	0.8	6.1	16.8	1.8	30.7
471	147.5595994579	7790	0.8	8.7	5.2	-8.4	1.1
472	147.1542020661	8274	0.4	-11.1	28.1	11.7	13.8
473	147.6284799656	13984	7.3	11.9	2.1	-4.6	5.8
474	148.2979602639	11556	0.9	-5.9	10.8	4.1	7.7
475	148.4507023248	12447	1.8	8.1	18.3	2.6	6.5
476	148.0537896579	12679	0.8	-14.3	1.5	6.8	0.9
477	148.5892440177	7352	2.5	33.4	11.3	111.5	4.9
478	148.2259897757	8274	0.5	-14.5	22.8	11.8	17.4
479	148.4380744553	8844	1.3	10.3	3.6	-8.8	6.4
480	148.2242516516	9574	1.1	-11.7	5.0	-31.8	6.0
481	149.7028075692	10949	1.5	-19.4	2.4	-16.9	0.8
482	149.0214376824	11567	1.1	-5.0	7.3	3.6	3.1

Track#	time (Days from 1983)	Object#	Sigma	ra bias	ra sd	dec bias	dec sd
483	149.8394279744	13609	1.4	-11.0	14.6	15.9	8.9
484	150.3111148550	11684	2.8	-10.3	1.2	12.6	1.1
485	150.2380958284	12787	0.9	-19.5	9.9	17.3	3.2
486	150.1974035253	13907	0.8	-2.4	17.1	-6.0	6.5
487	150.6008760723	4882	0.2	-7.3	7.4	8.4	3.6
488	150.1615550921	8274	0.6	-20.4	3.8	7.7	3.3
489	151.9981963924	12959	1.4	-16.2	5.1	-9.4	3.1
490	151.2117137490	13899	0.8	86.1	5.8	-3.1	1.8
491	151.3775870061	7485	2.9	2.2	10.5	-14.1	3.9
492	151.9278513321	8462	1.5	-14.1	4.0	-9.5	2.9
493	152.1006995339	2511	2.7	-15.5	15.9	103.2	6.9
494	152.2315390116	7641	1.1	4.5	6.0	-11.3	4.6
495	153.3796183539	11075	1.3	-4.7	1.6	-5.6	1.7
496	153.0248131240	13591	0.9	-7.2	14.1	-2.8	6.0
497	154.0337991479	10669	0.7	-16.8	8.6	3.4	4.2
498	154.0940028639	13390	1.2	-1.1	4.9	-4.8	5.3
499	158.3167059281	11553	0.4	-11.3	10.9	5.9	17.7
500	158.6478882052	12679	0.6	-2.4	17.5	5.3	3.2
501	158.2614509181	12851	6.1	-47.6	25.6	21.4	11.8
502	158.5789307588	11144	1.0	-9.9	8.6	-20.2	1.9
503	159.1040955779	10150	3.5	2.3	2.2	9.4	2.6
504	159.2595747586	10976	0.4	6.0	7.9	-1.2	3.2
505	159.0002068076	13609	1.6	-29.8	39.3	-27.8	7.5
506	160.1754792831	11474	1.3	-5.4	6.0	-0.8	11.8
507	160.1190046473	11690	1.0	-2.2	19.2	-5.1	8.7
508	160.1175597462	11144	1.0	-6.3	18.1	2.7	6.9
509	161.8875375610	11057	0.4	-2.6	2.9	-8.3	4.1
510	161.8884535997	11079	2.1	13.3	26.8	-6.6	28.3
511	161.6129190397	11847	2.3	-7.1	8.1	23.2	8.2
512	161.8872284689	11896	1.0	-12.1	3.1	-6.1	3.7
513	161.9570775117	12384	3.3	12.3	49.4	-23.2	81.1
514	161.4744895726	13591	1.4	12.8	9.2	-72.0	4.5
515	161.3956619135	7586	3.0	-14.0	1.7	0.0	2.2
516	161.9597933609	8600	1.1	9.5	37.7	11.1	32.2
517	162.8896776969	11896	1.0	-14.8	19.4	-5.6	20.6
518	162.4020623374	12134	0.8	-32.6	14.3	-9.1	7.3
519	162.5223438205	13069	4.7	-8.1	5.5	30.8	2.7
520	162.6747661270	13961	3.5	-137.2	37.6	-25.9	28.7
521	163.9642839803	10369	0.9	10.2	2.3	6.0	3.6
522	163.5244013894	13069	4.7	8.0	2.5	37.9	1.8
523	163.6737575120	8462	1.0	-18.0	12.7	-5.5	7.7
524	163.8221680133	8548	1.0	-7.4	3.6	-8.1	2.4
525	163.5349472595	8600	1.8	14.2	30.3	-9.6	21.0
526	164.8915857645	11896	1.0	-5.9	1.1	-4.8	2.7
527	164.4129589291	12134	0.8	-42.6	9.3	-42.9	3.3
528	164.8068494041	573	1.3	-13.8	3.3	5.0	3.6
529	165.5599923843	10684	1.0	-18.1	4.4	5.8	8.8
530	165.8730394639	10684	1.0	-12.9	6.9	-10.6	4.0
531	165.0327509064	11079	1.1	-9.8	9.1	-5.1	6.3
532	165.6066960759	13016	3.0	-7.8	7.8	-5.4	11.8
533	165.0350615980	6302	0.9	-4.2	0.9	-4.7	1.5
534	165.6249991759	750	2.3	-57.5	14.1	66.9	3.1
535	165.9459845384	7902	2.4	-17.0	16.6	-12.6	8.3
536	166.6186980197	11474	1.5	0.3	8.8	-6.3	9.8
537	166.1205097426	7738	0.5	-50.4	10.3	57.8	7.3
538	167.5313337131	12892	30.6	46.5	3.6	-32.1	2.8
539	168.8186662689	11690	0.6	-3.9	0.5	-0.1	0.2
540	169.8160216734	10684	0.8	-17.4	1.1	-7.5	1.1
541	170.0587752828	12512	1.1	5.0	7.4	-5.6	4.2
542	170.0570181889	12561	0.4	14.9	28.2	-17.4	6.5
543	170.6038408292	13637	2.0	-11.5	3.4	-6.7	1.8
544	171.2036875571	11075	0.6	-14.3	0.3	-1.9	0.2
545	171.4876183075	12906	0.7	-5.0	3.9	-1.7	3.2

Track#	time (Days from 1983)	Object#	Sigma	ra bias	ra sd	dec bias	dec sd
546	171.9683465971	9329	1.9	1.1	14.6	3.7	4.4
547	172.9072599521	10605	1.8	-10.0	0.4	29.1	1.5
548	172.2148529147	11862	0.9	-14.5	11.3	5.9	5.2
549	172.1432891588	12851	6.2	11.4	51.5	-9.8	29.4
550	172.3464032008	12986	0.8	19.6	5.8	-6.1	16.3
551	172.0610991363	13112	2.4	40.5	32.5	35.5	61.4
552	172.5627202003	13390	0.7	-12.6	4.4	4.9	3.5
553	172.2050518799	12547	0.9	-0.7	2.7	-4.2	2.6
554	173.2052936080	10155	1.3	10.1	11.6	-10.7	9.2
555	173.0613626424	10485	1.1	-2.0	11.2	1.9	17.3
556	173.9101323684	10605	4.6	2.9	7.0	29.2	5.9
557	173.6110239185	12339	1.0	0.1	18.3	-10.2	6.6
558	173.2962916584	13205	1.5	-12.2	3.7	4.5	1.8
559	174.9129027333	10605	5.4	24.4	4.3	52.5	14.9
560	174.6370688167	11474	1.1	-3.8	4.9	-0.2	6.9
561	174.3592870389	6058	2.3	-1.8	7.5	-5.9	3.1
562	175.6295711262	10369	0.9	5.6	5.7	-13.8	9.7
563	175.1380848925	11474	1.1	-4.4	4.5	-4.9	7.1
564	175.5686044494	13237	1.9	-1.3	6.7	3.3	11.7
565	175.2102928553	13253	0.3	-11.0	3.5	6.6	7.6
566	175.0793906521	14194	0.5	45.2	23.8	-13.2	12.3
567	175.9166155847	9049	0.3	-21.1	7.2	-34.3	12.4
568	176.4263378291	11556	0.9	5.8	10.1	-10.2	9.3
569	176.9184114178	12159	4.1	3.5	6.6	-11.0	8.6
570	176.1444751837	12561	0.6	-20.9	4.8	7.2	3.4
571	176.4972262569	8274	1.3	-4.5	1.3	3.9	0.4
572	176.0583426676	8548	1.0	-22.8	4.8	-16.5	6.2
573	176.6137983051	13137	40.0	-10.3	6.4	36.0	3.5
574	177.1329261539	11909	3.7	41.8	14.4	-3.3	25.8
575	177.1419973701	12133	1.4	1.6	8.3	-0.3	14.0
576	177.5035317275	8529	0.7	-0.4	4.3	-6.1	2.8
577	177.9034985280	8529	0.7	-18.2	5.2	-38.0	2.0
578	177.0836867370	8774	2.4	123.2	32.1	11.3	15.5
579	177.6341181965	13446	106.1	-61.0	0.4	54.3	0.9
580	178.3631286134	11075	0.5	-7.8	2.7	-2.5	0.9
581	178.9907680282	12159	3.9	-6.7	6.3	-12.7	6.5
582	178.4327195076	13390	1.0	-69.1	105.7	55.0	36.4
583	178.2983543914	14005	2.4	-2.2	10.6	2.6	4.7
584	178.7789809166	6916	0.9	-4.0	1.4	-1.0	5.2
585	178.8475682024	9647	1.1	-25.9	6.9	-21.2	6.8
586	178.0614727226	13295	1.5	-25.1	11.0	-20.4	13.6
587	178.5636455237	13295	1.5	-19.4	5.9	-13.6	5.2
588	179.5778626998	13383	1.2	0.0	17.6	-11.3	17.7
589	179.9888511080	7800	1.1	-6.7	2.5	-4.3	0.7
590	180.0789569729	13383	1.3	-3.2	9.8	-2.6	6.6
591	180.1595459428	13631	1.6	-28.6	3.4	18.5	1.6
592	180.0879788981	13652	0.9	-7.2	3.7	6.6	2.0
593	180.6334113001	9269	2.2	-17.1	6.2	-4.1	3.0
594	181.6254486462	12967	0.8	49.3	8.4	8.5	2.8
595	181.1614734116	13631	1.6	13.2	2.9	2.3	1.3
596	181.1343891747	9269	2.2	4.1	14.6	8.3	7.7
597	182.0924830963	12967	0.9	2.0	16.7	-6.4	6.4
598	182.3784001179	14005	2.5	11.9	12.7	3.5	6.3
599	182.5260939597	4354	1.7	-1.3	10.9	2.1	1.1
600	182.3128486672	7545	4.9	-5.8	5.8	1.2	4.0
601	182.0182889161	8529	0.8	0.0	4.0	-23.0	1.5
602	184.0965878017	11144	14.4	-41.5	10.8	-62.2	4.7
603	184.0243259206	11728	1.4	-40.5	1.6	2.8	0.2
604	184.4616431422	11791	0.9	12.6	1.1	37.5	3.0
605	184.0247906963	13431	2.9	-14.5	8.0	31.9	3.2
606	185.5187174689	12383	1.3	-1.3	7.9	-7.1	2.7
607	185.0181259394	8600	1.7	-3.7	21.6	3.0	11.2
608	186.3035095994	10485	0.8	-21.0	31.1	12.9	20.8

Track#	time (Days from 1983)	Object#	Sigma	ra bias	ra sd	dec bias	dec sd
609	186.0884471873	11509	1.6	2.7	95.0	-56.1	51.5
610	186.1627940374	8529	0.8	3.1	94.5	12.1	75.0
611	186.5916492130	8600	1.8	18.1	20.7	-6.7	13.9
612	186.6388104153	8840	9.0	26.8	10.4	-21.7	5.0
613	186.9233341062	14134	2.1	8.4	11.6	36.4	5.5
614	187.5965492832	11662	0.6	-15.7	8.7	-3.2	3.6
615	187.0909602104	12907	0.6	1.8	1.8	5.0	5.7
616	187.0223706352	12993	1.8	9.4	4.2	1.9	1.9
617	187.6047158922	7318	3.3	-34.3	2.7	3.1	0.8
618	187.3782485534	7372	4.4	189.1	0.1	-123.8	0.2
619	187.2496809822	7794	1.6	-4.9	5.2	4.7	1.4
620	188.8458849458	10684	1.4	-9.9	11.3	-32.0	4.5
621	188.5993890278	11662	0.9	-9.0	0.2	-1.7	1.0
622	188.0345207742	12556	2.0	-8.6	32.0	-20.4	21.8
623	188.5951258083	12907	0.6	4.4	14.3	2.5	20.0
624	188.3087029718	13080	1.3	11.6	5.8	-19.7	10.8
625	188.7944274153	13205	1.0	-22.4	15.2	3.5	19.5
626	188.5353502547	13890	0.9	-30.4	6.7	10.8	5.9
627	188.1669487485	6958	6.6	9.8	6.3	-9.1	7.1
628	188.1667404395	7903	1.9	-9.2	3.0	-1.6	2.3
629	188.2367268214	9574	0.8	-18.1	13.8	1.3	21.8
630	188.3797695057	9579	3.8	17.0	20.0	-40.6	57.4
631	188.3931655392	14114	0.8	-25.9	3.8	11.0	1.6
632	189.6012457815	11662	1.2	-1.7	11.3	-7.5	11.5
633	189.8511494557	11783	2.0	20.0	5.1	-16.6	2.5
634	189.5967624846	12907	0.6	2.8	12.9	11.1	26.2
635	189.5720034479	13269	0.9	-17.7	18.2	-7.7	6.7
636	190.6026822420	11662	1.7	6.6	2.6	-2.8	1.4
637	190.2324292236	12070	11.9	68.0	2.2	-3.8	3.1
638	190.3946922037	9017	5.0	-14.3	12.6	-3.1	4.0
639	190.3841181498	14182	0.9	-2.8	5.0	1.8	6.4
640	191.9394991444	10803	0.6	-20.4	2.5	-11.2	0.4
641	191.6036971473	11662	0.9	-9.2	3.4	-10.0	2.5
642	191.6047567346	11791	5.0	-40.3	1.1	5.6	1.5
643	191.4567688801	12627	2.4	6.3	1.3	12.8	2.3
644	191.0989707463	12907	0.6	-4.1	7.6	-1.3	9.8
645	191.2445604134	14034	0.7	-1.3	1.2	-2.1	7.0
646	191.6369653266	3212	1.1	-0.1	15.5	4.1	8.4
647	192.2385635740	12159	3.5	-32.0	10.8	-16.8	10.4
648	192.0168115928	8418	2.1	-4.2	13.4	-10.2	14.5
649	192.1128562360	12309	6.7	33.9	0.1	6.5	0.3
650	193.1049850250	10803	0.6	4.0	7.6	9.6	6.7
651	193.8820873319	10984	1.7	-9.4	0.7	-9.3	1.5
652	193.5369622417	13112	0.9	10.9	19.0	-2.4	19.6
653	193.5909425719	13295	1.0	-0.2	21.1	0.5	18.2
654	193.9531535091	13446	5.5	67.6	13.3	-0.4	24.6
655	193.3289582272	13900	1.9	-26.6	13.6	-14.2	5.0
656	193.8605482851	3212	0.9	-18.7	15.4	0.8	2.0
657	193.0927753279	829	2.5	-34.2	5.4	-4.4	4.5
658	193.9400825780	8840	1.1	-22.0	7.1	6.1	3.6
659	193.3935522292	9269	1.9	2.2	3.0	-8.4	1.4
660	193.5907301594	13298	3.5	-16.4	10.5	-14.6	7.5
661	194.6628763972	13295	1.5	-6.2	0.6	-4.2	0.6
662	194.1100932727	8741	1.3	10.1	0.1	14.6	1.2
663	194.6622615556	13298	3.5	-36.7	3.6	-27.1	1.4
664	195.2466954590	11073	0.5	-2.0	4.8	-3.1	8.9
665	195.5999746144	11602	4.2	8.5	14.5	-9.5	15.4
666	195.5997673297	13016	41.8	27.4	8.2	3.9	7.7
667	195.2331331692	14077	0.8	143.0	7.8	-42.9	3.0
668	195.6010727573	6939	2.8	-68.0	3.6	2.3	22.4
669	195.8130699161	8015	1.8	-1.7	5.3	-15.2	3.6
670	195.4762117677	13899	2.6	23.6	8.0	-7.1	3.2
671	196.0972868035	12086	4.9	-23.4	7.4	-51.5	4.6

Track#	time (Days from 1983)	Object#	Sigma	ra bias	ra sd	dec bias	dec sd
672	196.8653207459	13609	2.3	7.1	4.8	-5.8	4.6
673	196.7362769477	3315	0.6	-31.7	8.1	26.3	8.4
674	197.0946624803	12078	5.8	6.6	4.1	-9.2	0.9
675	197.9579994280	8195	3.7	8.5	19.3	82.1	38.0
676	198.6649325698	12078	6.2	20.7	12.2	-1.2	4.4
677	198.6016253635	6939	0.3	-52.3	71.4	61.5	100.1
678	198.8102435175	9007	1.4	-23.8	6.9	20.4	4.3
679	199.6258193185	10803	0.9	0.5	0.4	25.1	0.0
680	199.5592161981	12156	1.7	1.7	6.9	8.5	4.2
681	199.5909457355	8476	0.3	0.3	50.4	-16.3	36.7
682	200.9518198463	13878	2.2	-12.5	2.5	-17.4	0.8
683	200.0178093414	3307	1.2	18.0	11.7	34.3	10.1
684	200.6230652595	8548	1.2	-0.1	3.9	1.8	1.9
685	201.1033962191	13295	0.9	-18.6	2.3	-7.0	2.3
686	201.6044968155	13295	0.9	-5.9	1.8	2.5	2.1
687	201.5168893609	8546	0.9	-19.6	6.6	-13.7	3.6
688	202.9557224463	12471	1.8	-32.6	9.0	-13.7	3.8
689	202.5323613310	14195	3.8	36.4	1.5	-26.2	0.4
690	202.9675415170	8462	1.2	0.6	20.6	10.0	61.0
691	203.1969027546	10155	3.6	10.8	19.1	1.7	5.7
692	203.5552196544	11240	3.5	10.1	11.1	-2.1	5.2
693	203.5422851258	12078	6.1	2.2	7.2	-13.4	3.9
694	203.7549322787	13205	0.9	-2.9	0.4	7.7	17.5
695	203.0642337971	13652	38.6	-86.1	9.4	-1.8	3.0
696	203.6739302435	6779	1.6	-7.5	17.1	-28.8	7.8
697	203.1980034767	8548	1.2	2.1	7.0	-3.0	3.8
698	203.6052243067	7468	6.0	-30.5	0.9	-7.6	2.8
699	204.0626557060	10976	6.1	22.0	11.3	-10.4	4.2
700	204.9019663241	10984	1.2	-8.4	4.9	-0.2	13.9
701	204.5578443544	11240	3.5	-5.2	6.3	7.2	3.7
702	204.6074539174	12078	6.5	6.5	10.1	-14.0	4.7
703	204.4188506103	12561	3.2	5.5	4.7	-48.2	0.4
704	204.0660362612	12850	1.1	-4.4	7.4	11.0	2.7
705	204.1112329539	13075	8.1	-23.6	11.1	-37.4	10.6
706	204.2030177360	13390	2.2	14.6	20.9	3.1	36.2
707	204.7541069677	3315	2.4	-33.9	9.6	8.5	8.1
708	204.1118230218	7373	1.3	-10.0	4.1	-18.1	4.0
709	204.5590596863	9269	1.3	8.0	4.4	-7.2	2.0
710	205.5606941170	11240	2.8	5.2	2.2	-9.9	0.2
711	205.4983564779	11440	1.6	-55.1	6.0	30.7	2.7
712	205.8336209133	11896	3.1	9.7	2.7	10.8	5.1
713	205.6048897771	12850	1.1	-12.6	12.1	-12.2	5.1
714	205.6050957804	12967	2.5	22.3	11.7	-10.7	5.1
715	205.5676405257	7376	1.6	-13.9	5.2	-6.8	1.5
716	205.0456551220	7382	1.2	-17.1	5.9	-23.4	6.8
717	205.5026386435	7545	17.7	-12.2	28.5	4.3	8.9
718	206.6076692219	12967	1.0	-9.4	9.6	-12.2	4.3
719	206.2956340594	3173	0.6	-9.1	2.9	11.3	1.6
720	206.8345201361	8418	1.4	-20.9	1.7	-20.7	1.4
721	207.9092803375	10315	0.7	-17.7	33.0	-1.6	20.3
722	207.0645500992	11240	2.7	-4.8	7.1	-2.8	4.5
723	207.2849150593	12547	0.9	9.3	7.6	-7.5	3.5
724	207.1037715822	898	0.4	-0.2	9.4	-64.4	4.0
725	207.6323558326	9647	1.4	-23.9	12.1	28.2	11.3
726	207.9078552994	9889	0.9	-10.7	8.1	-12.7	8.7
727	208.4925124831	10949	1.5	-17.0	11.7	10.6	38.2
728	208.0671582956	11240	1.8	-0.9	0.2	-7.2	0.1
729	208.7687427532	11909	2.7	3.3	6.0	-18.9	7.9
730	208.0714353995	12827	2.5	9.9	7.3	-28.5	4.1
731	208.4945233670	14206	0.6	-3.1	5.7	-2.1	4.3
732	208.5453792587	3029	3.1	-30.8	7.6	-7.8	2.6
733	208.6379513175	9049	1.2	-19.3	1.6	5.3	8.3
734	209.0685499826	11240	1.7	24.6	19.4	-15.0	40.4

Track#	time (Days from 1983)	Object#	Sigma	ra bias	ra sd	dec bias	dec sd
735	209.5026426050	12561	0.9	3.2	2.7	-8.0	4.7
736	209.9124632253	13012	1.8	-0.2	1.8	3.9	2.0
737	209.0776951043	13954	2.1	-28.6	1.6	24.7	0.6
738	209.1388113604	9049	1.2	-12.0	23.1	5.6	23.9
739	209.7618588102	9329	5.5	-11.6	16.9	-34.3	5.9
740	210.2923907859	11684	3.2	22.8	9.0	-5.9	2.9
741	210.7593145816	13907	3.4	0.8	5.2	-38.2	2.2
742	210.3620317207	163	1.6	-33.3	21.1	31.5	3.1
743	210.3784608380	3212	0.7	-19.7	1.0	3.4	2.2
744	210.8342326376	7468	9.5	32.9	10.9	23.9	5.8
745	210.5532418785	8751	2.1	-5.9	1.2	-23.2	0.5
746	211.1172418366	11256	1.8	2.7	0.8	-32.9	1.8
747	211.1509567823	11941	1.9	-0.7	7.3	8.0	2.1
748	211.9768289238	5816	5.5	46.7	9.2	-27.0	3.8
749	211.0038636358	746	2.8	33.9	18.4	96.8	5.2
750	213.0833882331	13900	4.9	-17.7	21.1	20.8	29.6
751	214.5904326319	8331	1.8	-15.2	11.6	8.3	4.2
752	214.5901576505	7545	17.7	-18.4	8.8	3.1	4.7
753	215.9914211128	13432	2.7	-8.7	8.1	-3.8	2.6
754	215.7802267760	4966	2.2	-41.1	2.1	2.8	4.8
755	216.5584937190	11153	2.0	25.5	9.4	-125.8	2.9
756	216.1405610993	12833	2.5	-23.1	2.5	-7.6	2.6
757	216.8341884684	13609	0.6	97.7	33.8	6.3	74.6
758	216.8407468919	14115	0.7	-3.5	8.4	-9.2	3.5
759	216.6264632016	14158	3.1	11.2	9.2	1.3	3.3
760	217.9918998229	13890	0.8	-15.2	1.1	-9.1	4.5
761	217.0918730102	7318	5.7	17.2	4.7	15.0	1.0
762	218.5659444578	2206	0.7	-45.9	9.5	13.8	3.8
763	219.4456847823	12159	1.1	17.6	11.4	0.9	5.3
764	219.5379496181	13610	7.5	-27.5	11.0	53.6	6.9
765	219.9247451637	5615	0.7	-25.2	72.6	52.2	35.4
766	219.1713291161	7545	1.3	24.2	9.9	-4.4	3.6
767	219.4437488419	7653	3.3	35.3	4.0	-20.2	1.0
768	219.7076417605	8751	2.3	-8.9	18.2	-17.8	5.4
769	219.7058477238	9506	2.3	-13.4	7.3	36.9	2.3
770	219.2332397554	14034	2.2	-2.9	7.8	-4.4	3.8
771	220.0279734256	13900	4.8	-38.2	10.4	16.9	3.8
772	220.7051039751	4630	1.7	90.5	17.7	-95.0	4.6
773	220.1383674440	5816	6.4	30.1	12.3	-15.2	5.8
774	220.6339888324	6052	1.2	29.3	1.2	3.1	0.1
775	221.9326576736	10315	0.6	7.5	23.6	-3.1	20.1
776	221.8648339556	10605	1.5	19.7	0.5	-17.0	2.5
777	221.8632222737	11896	1.7	-9.6	8.1	-8.3	9.0
778	221.9932990676	8134	8.0	31.5	5.2	-21.7	2.7
779	221.5194761660	8274	4.6	12.5	6.8	-8.7	5.6
780	221.8626426119	8701	1.7	-13.4	2.1	-4.6	3.3
781	221.3093048818	9506	2.3	-26.3	5.7	-55.3	2.3
782	222.0320906316	10669	2.1	-28.0	4.3	11.8	1.0
783	222.9372612530	11555	2.7	-20.0	6.3	-21.7	12.3
784	222.0324208834	12065	3.9	-14.6	14.9	1.8	34.7
785	222.9344026552	13012	1.7	-15.1	3.5	-5.8	2.2
786	222.0280441738	6058	1.5	-3.3	1.4	1.0	0.6
787	222.3095526622	9506	0.8	72.6	5.7	94.1	2.2
788	222.9936602248	9889	0.8	-1.8	4.6	8.8	4.9
789	223.8683198137	11589	2.1	-13.7	2.5	-15.6	2.4
790	223.5823962666	11909	0.9	-25.9	7.7	-23.8	8.3
791	223.7952560848	14258	0.6	-15.9	7.9	-7.1	7.6
792	223.5382254735	8822	6.3	-63.9	42.0	101.2	9.1
793	223.9947797958	9889	0.8	-16.6	10.1	4.8	11.5
794	224.2491911838	12562	0.8	-59.3	3.4	-6.2	1.2
795	224.5854048285	12833	6.5	52.5	0.9	-26.2	1.0
796	224.0342424714	13069	7.7	0.9	7.1	47.0	1.9
797	224.8636814866	16	0.6	-11.6	25.5	14.3	0.3

Track#	time (Days from 1983)	Object#	Sigma	ra bias	ra sd	dec bias	dec sd
798	225.7295438780	11602	2.6	-37.0	16.7	-36.6	15.0
799	225.7175943164	14086	4.1	5.9	1.5	4.9	1.6
800	225.5825233834	340	0.6	-21.1	5.0	12.6	0.4
801	225.9451417845	8195	1.6	-4.5	28.5	-12.5	10.6
802	225.5743427115	8774	9.9	6.5	3.7	35.8	0.2
803	226.9463719852	10605	6.7	-33.0	15.3	-30.1	17.4
804	226.7285720873	11909	1.0	-39.5	10.2	-16.7	4.7
805	226.3287337509	13603	2.0	-50.1	1.5	37.5	0.6
806	226.7947593034	11661	1.9	-10.5	5.3	8.5	11.7
807	227.5861549729	14259	0.6	-33.7	9.6	-8.2	2.3
808	227.9417438193	6779	0.9	-26.3	32.1	-10.5	19.3
809	227.5791235262	9931	5.8	26.9	0.9	-41.3	3.2
810	227.5862709411	14260	3.1	-14.0	5.2	-3.5	1.3
811	228.7238836762	11728	5.3	8.9	9.9	8.2	2.8
812	228.5814088803	14195	6.3	40.9	12.7	-27.5	8.3
813	228.5815589910	8774	12.3	-26.0	7.4	33.1	2.4
814	228.0133574657	8820	0.4	-31.0	17.4	-9.7	5.4
815	228.5946959338	9921	1.5	-21.0	11.3	-11.0	10.5
816	229.2305201023	11142	1.2	-17.0	6.1	2.3	4.4
817	229.0144088795	11896	1.7	-46.5	8.8	-14.2	4.4
818	229.6443473499	4790	1.2	-28.2	15.0	7.2	4.4
819	229.9432165677	8751	2.9	-10.1	1.5	-14.9	0.4
820	230.0937925620	12070	9.3	18.8	46.6	2.2	41.9
821	230.1888310523	12471	7.2	-5.4	2.7	-12.4	0.4
822	230.1834892219	2364	3.3	-3.6	5.4	-6.1	18.8
823	230.4076260354	2933	1.4	-22.9	26.6	-41.0	1.2
824	231.6294819856	10960	1.8	12.0	1.6	32.6	0.9
825	231.5586746465	14264	1.3	-22.7	20.2	22.3	13.7
826	232.6184955682	13940	5.2	3.5	1.9	-3.7	1.3
827	232.8021879198	829	2.3	-46.4	7.0	27.9	0.9
828	233.8867604312	11856	2.0	-7.3	9.0	-4.3	9.4
829	233.7380504431	12940	5.0	-20.8	17.1	-58.3	8.9
830	233.0514510807	13899	6.0	-3.2	5.6	0.4	1.7
831	233.3345615560	6058	1.0	2.6	8.0	0.3	1.4
832	233.0984164105	8601	10.2	123.5	2.9	-67.3	2.7
833	234.2735166090	10025	1.4	-9.8	3.5	7.4	2.0
834	234.8115060314	11661	1.5	13.3	3.7	-3.0	4.4
835	234.0608480252	13610	6.0	-17.0	7.5	8.2	2.8
836	234.1940927549	13913	0.9	9.1	3.1	16.4	1.5
837	234.1227765816	7794	0.5	8.9	22.0	-6.7	7.5
838	235.8916175852	11328	0.3	4.6	2.2	30.2	2.5
839	235.1277842792	11676	5.0	-2.2	6.1	11.4	1.8
840	235.2657367203	14034	1.0	1.4	5.9	-4.0	1.0
841	235.7443455642	9927	1.9	-5.3	4.7	0.8	2.6
842	235.4140438976	14114	0.8	3.7	19.9	-5.3	10.6
843	236.2722253656	10960	0.7	-7.1	12.2	-1.2	3.4
844	236.4161765498	11728	3.8	-17.3	6.1	-10.7	2.6
845	236.5326750199	14264	2.0	-13.2	21.7	-18.8	4.9
846	237.6805827072	13075	3.2	-13.3	6.4	-47.4	4.9
847	237.6780052398	13897	2.4	-16.7	1.4	-18.4	1.6
848	237.9569890491	14264	1.5	-20.5	2.7	-14.2	1.1
849	237.8880664689	5816	4.7	-8.0	10.0	-22.7	3.2
850	237.0308302316	7583	3.1	14.2	16.4	26.7	5.5
851	237.4203308317	8331	1.0	1.7	20.4	-3.5	5.2
852	238.5535188277	12156	1.3	0.4	25.7	-7.2	11.6
853	238.9631872171	13964	0.8	-21.4	4.1	-10.9	1.6
854	238.5407038685	2389	1.1	-22.5	1.6	37.7	5.0
855	238.1294233277	628	2.3	-11.0	1.7	35.4	2.4
856	238.6261057709	9889	1.6	54.7	8.8	28.0	2.9
857	239.1155235501	11073	0.7	-10.7	1.9	-2.2	4.6
858	239.4857437543	8492	1.4	-10.9	7.1	-5.6	3.5
859	240.1396417573	10893	0.9	-3.8	3.2	0.6	1.3
860	240.4168457199	11240	1.7	4.5	8.9	2.2	4.2

Track#	time (Days from 1983)	Object#	Sigma	ra bias	ra sd	dec bias	dec sd
861	240.0381406466	13446	0.7	1.2	8.9	-12.3	1.4
862	240.4258009262	2643	0.5	1.3	16.2	14.5	3.3
863	240.4876200546	8492	1.2	1.2	11.8	4.8	8.0
864	240.0647060036	9506	3.2	-4.2	7.6	7.0	0.1
865	241.4908379145	10696	1.0	23.7	1.4	4.3	0.2
866	241.3481030794	14206	1.4	22.4	5.5	14.4	0.4
867	241.4390071193	3212	0.5	-13.6	1.4	1.7	4.2
868	242.4924726534	10696	0.8	-49.8	64.3	-27.7	41.1
869	242.0689409823	13913	1.3	24.1	7.1	5.8	0.1
870	242.3484108610	8600	1.3	0.1	12.0	2.7	4.7
871	243.9114032510	13960	1.1	-26.0	35.3	7.7	16.6
872	243.6892614595	503	1.5	-59.0	20.8	77.2	19.7
873	243.8413344182	7276	1.5	-16.0	0.7	0.6	14.0
874	243.4934953253	9635	1.0	12.9	3.7	8.0	1.6
875	243.9692672201	14277	1.0	8.3	52.2	5.3	29.3
876	244.4336262894	11571	0.3	-10.0	3.6	5.1	0.2
877	244.9716311623	13012	1.3	-34.7	6.4	-10.2	1.6
878	244.1456918634	608	0.9	18.1	14.0	-4.3	13.9
879	245.8338110965	10369	2.3	-20.8	7.7	-19.8	3.6
880	245.8413084559	13012	1.1	-11.3	9.4	-11.3	15.4
881	245.1610971363	14264	1.8	4.8	1.5	22.8	3.5
882	245.8184564906	2877	2.2	37.5	19.1	83.9	7.5
883	246.0625707875	2150	0.8	-16.5	3.6	-16.7	7.2
884	246.6324499648	9921	1.8	-1.9	1.4	-11.8	7.8
885	248.1338175725	12940	2.5	-79.3	1.8	15.0	11.4
886	248.7765477992	13012	1.4	-17.0	2.1	-14.6	8.7
887	248.7634533640	13899	6.3	-46.3	2.0	-6.7	0.4
888	249.9753991601	13012	1.1	-29.3	20.5	12.4	17.1
889	249.1365678713	14264	1.5	-32.1	0.4	-14.0	1.6
890	249.1247010308	4966	51.2	-121.6	13.2	115.3	2.1
891	249.5040693997	7903	0.8	19.8	1.4	-8.0	0.7
892	250.5203364310	10422	0.8	63.9	11.0	51.7	5.8
893	250.5203079175	10423	1.1	-5.5	2.9	1.8	1.5
894	250.1367219852	11861	1.1	5.2	21.2	-17.9	36.4
895	250.7681472012	12933	2.0	-16.8	2.3	-8.3	0.6
896	250.7691882001	503	1.4	-96.2	30.5	81.5	7.3
897	250.6314838707	6302	0.4	-9.1	20.6	-9.1	14.7
898	251.8514686336	11589	1.0	-13.4	2.3	-3.0	1.7
899	251.9984346054	11909	2.5	-13.8	0.3	-33.8	3.3
900	251.4473480985	13909	1.8	17.5	33.8	-14.9	8.5
901	251.6417700980	13967	1.5	-35.2	2.7	-17.3	20.3
902	251.3768467082	14258	0.9	-3.3	1.9	-0.7	0.5
903	251.4367338375	8548	2.0	-1.3	7.9	-16.3	6.1
904	252.7851925661	11328	0.3	-10.5	1.7	-24.5	23.1
905	252.7840843366	11589	1.1	12.7	39.4	-20.5	8.8
906	252.1462741936	12159	4.4	8.0	12.0	-42.7	23.5
907	252.8468890450	5816	1.7	-1.8	6.3	-15.6	3.3
908	252.5882248262	7794	0.3	3.7	11.8	0.7	0.7
909	253.3126865999	10894	0.9	-24.8	3.6	7.2	2.2
910	253.1451592775	11602	0.8	-10.9	0.4	-24.1	0.2
911	253.7825751422	11602	0.8	-36.1	25.3	-21.8	17.6
912	253.0010343042	11909	2.5	-11.6	2.7	-23.6	7.1
913	253.1487101053	12156	1.4	-8.2	4.5	-16.5	4.1
914	253.7898018940	14259	1.6	-7.2	3.9	-15.5	7.8
915	253.7859583785	14313	0.9	-18.0	1.8	-10.1	3.3
916	253.9944295700	7583	1.3	-13.7	8.7	2.3	4.6
917	253.0551213535	8134	2.1	-21.5	27.6	3.3	3.2
918	253.6454499220	9506	2.4	-11.7	0.7	-13.0	0.6
919	254.9300605627	14319	0.2	7.8	43.4	-12.0	68.8
920	254.9965990929	7583	1.7	4.3	1.0	-4.6	0.4
921	255.8615344385	8195	1.3	-17.0	1.0	-11.4	8.5
922	255.7910906839	9911	3.6	-10.2	1.6	-30.5	10.3
923	256.6538034315	10803	2.6	16.6	3.4	-25.2	3.3

Track#	time (Days from 1983)	Object#	Sigma	ra bias	ra sd	dec bias	dec sd
924	256.0088955234	11909	0.5	-3.4	2.0	-29.3	2.8
925	256.7917845250	12066	1.2	-12.7	1.4	-3.2	3.2
926	256.6538408456	14260	2.0	49.0	17.8	-56.7	12.3
927	256.6538034315	10803	2.6	16.6	3.4	-25.2	3.3
928	257.6554021863	11589	1.1	-3.6	7.3	-14.3	9.8
929	257.0108684157	7382	1.1	-8.3	8.5	-19.3	12.6
930	258.1739066059	11862	1.4	-17.9	2.0	12.9	1.0
931	258.5628062958	12940	2.3	-42.3	0.2	-26.1	1.2
932	258.8725022416	13967	0.4	6.8	3.1	-29.5	3.3
933	258.5704843985	14158	1.4	-16.5	11.8	-11.8	2.4
934	258.9344825765	14313	0.9	-13.6	5.7	1.8	3.5
935	259.4560584289	10315	0.4	29.8	5.6	28.2	1.5
936	259.8682245153	11328	3.2	-25.0	1.7	-15.6	2.8
937	259.8684385957	11384	1.3	-23.2	1.5	-8.5	4.5
938	259.5842201642	11554	2.1	-59.4	1.6	-49.6	1.6
939	259.0093481307	13075	0.7	-13.6	7.7	-7.9	9.6
940	259.5236694899	8187	1.0	8.4	1.6	-4.2	1.0
941	259.0640178759	9843	0.4	-22.9	29.7	22.1	12.7
942	261.4551060990	12156	1.2	-7.2	6.3	-11.6	3.4
943	261.5262410235	9635	1.0	45.8	44.4	35.9	89.7
944	262.4591145009	10455	1.4	9.1	5.2	0.7	1.3
945	262.5957573929	13964	1.2	1.0	5.5	-16.9	4.3
946	262.3233811375	14034	1.6	-2.5	23.5	4.3	21.0
947	263.4621049108	10455	1.4	41.0	21.1	6.7	5.3
948	263.8754602215	13875	1.1	-34.4	9.3	-14.1	9.5
949	263.0129008525	7738	2.2	-51.8	8.1	-14.4	1.0
950	264.4644330162	13237	1.3	11.3	16.8	-13.1	27.9
951	264.5790546088	14195	10.1	-33.0	2.3	33.3	0.4
952	264.9482075866	7780	0.9	-28.8	0.2	-12.6	1.2
953	264.3911375821	9495	0.4	7.3	0.5	-87.2	0.6
954	265.3946187932	13253	3.6	0.6	6.4	12.4	1.8
955	265.5810260469	14158	0.9	-36.9	5.9	27.9	1.3
956	265.3959308987	7372	0.4	14.5	3.2	9.5	0.6
957	265.5567781656	831	1.7	-38.6	11.7	28.2	21.9
958	265.8792716890	9921	1.4	-5.0	17.1	13.9	12.8
959	266.2506244233	11509	3.0	40.4	9.2	4.0	3.7
960	266.8101137110	2861	2.1	-25.2	7.0	12.8	3.5
961	267.9627122241	11073	2.4	44.6	7.8	-3.1	4.0
962	267.3264845069	11871	2.9	-48.9	4.7	2.4	1.4
963	267.5898057146	13912	0.9	-103.8	30.1	-17.6	1.4
964	268.8839949564	11758	1.3	-27.9	2.0	-2.1	1.5
965	268.9559496881	7373	1.3	4.6	8.7	73.0	4.3
966	268.9561771876	9880	1.4	-93.7	0.8	-7.5	0.0
967	269.1238267244	11567	1.9	-31.2	9.3	5.2	1.9
968	269.6799717251	6939	1.3	10.5	6.6	-34.1	3.9
969	270.4000708512	12959	1.3	8.4	8.0	1.5	3.4
970	271.4020082716	12959	1.3	15.6	5.9	2.6	2.8
971	272.4842860898	10455	0.8	-33.1	7.7	-12.6	2.1
972	272.1223687826	11888	0.3	-20.8	6.0	6.3	1.1
973	272.4039270413	12959	1.4	-1.7	17.9	-3.7	12.5
974	273.2655419384	11509	0.7	-4.7	6.4	-17.5	1.8
975	273.4058471646	12959	1.1	16.8	2.1	1.4	1.6
976	273.8221440088	13075	1.8	-28.0	2.1	10.4	2.1
977	274.8940500678	11758	0.7	-28.4	5.2	3.4	1.9
978	274.8957489178	11856	1.5	-19.0	13.4	-1.0	17.3
979	274.8143752564	13169	0.9	-9.2	0.7	2.1	2.1
980	274.8954901681	13897	1.2	-100.0	81.8	-37.1	26.2
981	274.0598352459	14130	0.4	5.8	3.7	29.6	0.2
982	274.4804184801	7653	0.5	12.5	9.6	-4.5	6.7
983	275.3449627959	12834	0.7	-46.4	16.5	-3.3	1.7
984	275.4100286140	12986	0.9	43.9	4.4	-17.2	6.5
985	276.9695764698	11384	1.4	-14.4	14.8	6.8	3.0
986	276.8247192060	11670	1.7	48.1	3.7	42.1	1.9

Track#	time (Days from 1983)	Object#	Sigma	ra bias	ra sd	dec bias	dec sd
987	276.5044907612	11783	0.9	-7.4	6.5	1.1	4.8
988	276.4194302086	11871	1.6	-10.1	6.4	2.1	0.7
989	276.1058993032	5816	0.5	-33.0	8.8	-0.9	1.8
990	276.4331863476	8822	0.8	-63.6	3.9	58.1	1.8
991	276.8924720162	9933	4.1	-93.2	21.5	63.4	5.9
992	277.4874918532	11896	1.2	-7.8	6.1	-6.4	1.9
993	277.9006448476	12915	1.2	-24.4	6.1	7.3	1.9
994	277.1360426883	13911	1.9	-119.4	14.8	-37.8	1.7
995	277.9532534755	14264	1.0	-22.3	2.7	8.2	1.3
996	277.8897048111	8368	1.3	-23.3	2.4	31.5	26.9
997	278.2759181231	11550	2.0	-7.8	6.8	-10.0	0.2
998	278.2732971778	7382	0.2	4.8	4.5	-12.0	0.2
999	278.9749693042	9829	1.3	-18.6	1.8	5.3	0.1
1000	279.1337486848	13080	1.9	41.1	63.1	10.3	9.2
1001	280.4935645363	11589	1.9	8.4	4.4	-1.0	3.0
1002	280.0449516711	11762	2.3	-25.7	10.2	-71.0	0.3
1003	280.0607740374	12993	1.1	39.6	44.4	2.0	14.2
1004	280.6187104924	13205	0.1	-81.9	7.7	0.3	2.0
1005	280.5617882512	8521	3.5	-85.8	10.5	40.4	5.5
1006	281.4938649259	10925	1.3	-6.0	4.8	-2.7	1.7
1007	281.3515730025	11909	0.3	-17.3	3.4	-11.7	0.9
1008	281.4923400752	12159	0.4	4.3	7.6	-2.5	4.6
1009	281.4315938446	12834	0.7	-28.9	5.7	2.7	1.8
1010	281.3084349939	2511	1.8	-38.6	22.7	-13.1	20.3
1011	281.5710137760	7794	1.5	-20.2	9.1	-0.7	0.9
1012	281.9805292398	9941	1.6	-29.2	9.1	6.7	1.2
1013	282.4958731824	10925	1.5	15.5	2.9	-14.1	1.0
1014	282.9800019066	13875	2.0	-16.9	0.5	6.1	1.1
1015	282.0453381400	5816	2.0	-34.2	10.4	2.6	1.5
1016	282.0468248890	8418	7.7	-4.5	3.6	44.1	1.1
1017	283.6146908250	14195	5.2	-10.0	3.2	-0.1	0.2
1018	283.6056265424	14258	1.4	14.3	3.7	-11.3	2.8
1019	283.0528457662	8741	5.2	-54.9	2.2	-41.9	0.2
1020	284.1220318172	11762	3.0	-37.0	7.9	-4.5	0.7
1021	284.6165350201	14195	5.2	-5.0	4.1	-1.8	2.1
1022	284.0699100398	7354	1.7	10.2	6.4	-9.6	2.3
1023	284.0684331375	8521	3.5	24.1	26.8	21.5	16.8
1024	284.4976275568	9049	0.8	19.7	14.7	-1.0	7.2
1025	285.1217929936	6779	0.5	-23.8	1.8	3.0	0.6
1026	285.0548179126	7000	1.2	2.8	3.0	19.6	0.1
1027	285.8404724862	7373	1.5	-28.0	13.0	18.4	0.9
1028	287.9200307845	12563	0.3	-67.2	1.8	5.9	0.1
1029	287.9845019425	5816	1.1	-1.9	5.4	1.0	1.4
1030	288.3709464681	11509	1.3	24.8	5.7	-40.8	0.6
1031	288.1580775360	11705	0.7	20.7	3.8	17.9	2.5
1032	288.9897482012	12915	2.2	-31.5	11.2	3.3	8.3
1033	289.1395469345	10089	3.9	-6.2	2.1	22.2	0.8
1034	289.4351046183	12627	1.3	16.8	5.8	7.3	4.1
1035	289.4367060244	12959	2.3	12.5	4.1	6.0	1.9
1036	289.2937799449	7369	0.9	167.5	3.7	21.5	0.5
1037	289.5931965977	8621	1.2	-22.8	3.9	3.9	2.9
1038	290.1550562244	11556	1.1	7.1	1.1	-3.6	0.8
1039	290.0922654149	13658	1.0	-22.8	3.6	3.2	2.9
1040	291.1562223947	12984	1.1	24.4	14.3	-6.6	23.4
1041	291.1422549770	11670	2.8	-4.3	1.1	-16.5	0.3
1042	292.6088477036	10893	1.4	-18.7	40.6	13.0	7.9
1043	292.3738680687	11076	0.9	-30.3	71.6	-29.0	40.6
1044	292.5225518751	11550	2.0	-23.7	8.1	-6.0	0.2
1045	292.4570936050	11871	2.6	-27.6	10.1	-8.4	6.2
1046	292.2253190933	6939	0.8	-16.3	20.4	-17.1	13.4
1047	293.5187366800	738	2.8	22.0	7.2	13.3	16.5
1048	293.6442337641	7629	0.6	10.8	2.1	-17.5	0.3
1049	293.6295097650	8840	1.3	-4.6	20.8	-8.3	0.9

Track#	time (Days from 1983)	Object#	Sigma	ra bias	ra sd	dec bias	dec sd
1050	294.4460550535	12512	1.9	11.3	1.9	0.1	0.4
1051	294.5770049547	12563	1.8	-36.7	7.8	16.5	1.5
1052	294.7839840295	13882	0.7	-18.4	4.5	5.0	1.3
1053	294.5193409186	575	1.0	-22.1	27.7	-14.4	11.2
1054	294.1153973329	631	1.1	-73.9	17.0	41.6	32.9
1055	294.5767126556	7625	0.9	-16.8	27.0	-13.3	22.4
1056	294.5155426270	8529	2.4	25.4	18.0	4.9	9.3
1057	295.4531509686	11076	0.9	-6.8	24.6	-9.3	1.9
1058	295.6487619981	7738	1.4	-21.3	3.5	34.5	2.4
1059	296.9302418617	11555	2.6	-27.4	2.7	16.4	0.3
1060	296.9944457565	14369	0.6	-22.8	15.8	0.8	6.2
1061	296.6505885428	7738	1.8	-26.1	27.1	31.0	11.9
1062	296.9925518071	7780	1.3	12.4	7.7	-25.2	15.3
1063	297.0980979083	11705	0.3	-34.5	27.2	-51.7	7.8
1064	297.2468523733	14194	0.7	-32.1	4.9	-10.4	0.7
1065	297.3816851093	14319	2.7	-79.2	1.4	-119.4	2.4
1066	298.0794314422	10092	1.9	-13.5	8.3	13.2	1.2
1067	298.8644517831	10485	0.4	-35.6	2.8	17.6	0.8
1068	298.0661240832	10950	0.8	-26.8	7.2	58.1	5.5
1069	298.1723130164	12984	1.0	-38.6	59.6	22.7	26.6
1070	298.5230360086	14206	1.5	2.7	12.1	-13.7	9.4
1071	298.6542296756	7738	1.5	-19.1	3.5	29.0	0.8
1072	298.5227191622	9506	0.2	83.1	7.1	40.8	1.8
1073	299.5742655669	10002	0.6	-11.1	3.6	-0.6	0.6
1074	299.5838851436	10092	2.2	-18.1	3.2	7.7	1.1
1075	299.4624899559	12311	0.6	-17.6	7.9	-10.5	1.8
1076	299.5860479163	13112	5.3	-58.1	13.0	25.3	9.8
1077	299.0105102500	13890	1.7	-16.7	8.8	14.2	0.2
1078	299.6557339891	6958	1.8	-26.1	8.7	23.8	3.7
1079	299.6559780884	7000	3.4	-26.6	7.4	16.4	4.3
1080	299.6560333860	7738	1.6	-26.7	3.1	35.0	0.3
1081	300.6578062198	7738	1.5	-41.0	36.4	41.7	11.0
1082	301.2445727397	10802	0.8	12.8	7.2	1.7	0.6
1083	301.5291784181	12376	1.6	4.9	1.0	2.2	0.3
1084	301.4579544725	12384	1.0	-7.7	1.6	-12.1	0.5
1085	301.3279360428	13090	1.6	-19.0	3.8	-3.7	2.0
1086	301.1021076037	2403	1.0	-24.3	1.9	21.8	4.6
1087	301.4575131344	6302	1.7	-6.8	2.9	-21.2	1.8
1088	302.5302240314	11073	1.0	25.3	3.6	6.9	0.5
1089	302.4594758897	11896	1.8	3.6	2.6	-9.0	0.7
1090	302.2449906083	11909	1.8	-3.2	14.3	-17.0	8.8
1091	302.2476495583	12519	0.9	8.5	2.8	1.8	0.7
1092	303.5917933935	10150	1.1	-4.6	4.7	2.6	0.5
1093	303.9498516469	10970	4.3	-20.4	26.8	0.7	31.3
1094	303.3185983144	12680	1.2	4.8	3.0	-7.3	0.8
1095	304.0928391253	10150	1.1	-18.1	1.2	10.5	1.4
1096	304.0872494848	7480	1.4	-24.9	3.4	13.5	0.5
1097	304.5882567337	7480	1.4	3.6	6.3	1.2	1.5
1098	305.8698240198	10002	0.8	-4.6	2.5	2.8	3.3
1099	305.8810976727	11075	1.1	-26.4	5.9	19.0	2.8
1100	305.1094785564	12134	1.6	-10.0	1.6	-4.8	0.6
1101	305.9531923962	12383	2.4	-22.6	1.2	11.6	0.1
1102	306.2509525231	10803	1.3	-4.4	8.5	-12.3	4.1
1103	306.3943493712	8548	2.2	6.6	7.0	-11.2	3.8
1104	306.5979838650	8820	0.7	-14.1	12.0	9.8	8.8
1105	307.4684542104	11589	2.0	-6.7	1.9	-11.4	1.0
1106	307.4677601749	12159	1.2	-12.6	15.9	-17.0	6.4
1107	307.9677995568	13446	2.6	10.3	10.9	1.9	13.3
1108	307.3364438686	13970	3.2	-45.2	1.1	-0.1	0.7
1109	307.6707373582	7000	2.8	-17.0	5.9	-51.4	4.0
1110	307.5521253411	7318	0.3	-22.0	2.4	10.7	1.6
1111	307.0382742524	9269	1.3	13.1	4.5	-0.3	2.9
1112	308.0153732492	13215	0.6	-17.4	8.5	14.6	2.4

Track#	time (Days from 1983)	Object#	Sigma	ra bias	ra sd	dec bias	dec sd
1113	308.9641510543	2796	3.3	-61.6	19.7	-105.8	31.4
1114	308.6716774431	7178	1.8	-10.6	8.4	6.7	3.6
1115	309.6653937752	10779	2.8	-31.9	8.0	11.0	7.7
1116	309.8012037438	7373	1.2	-89.3	6.7	106.5	26.5
1117	309.1026110690	8820	0.6	-7.4	7.5	8.6	6.4
1118	310.4725150443	6916	1.2	-165.7	4.3	-67.4	2.2
1119	311.1055671385	10455	2.2	-9.2	1.5	5.3	1.1
1120	311.0335584211	12368	1.5	10.6	11.9	-1.3	10.1
1121	311.6677164571	5816	2.6	-76.3	2.3	55.5	0.3
1122	311.6719480280	8274	3.0	-7.9	6.4	4.5	2.5
1123	311.6064343891	9411	1.7	-4.9	4.5	20.4	2.4
1124	311.6758217008	9574	1.2	-18.2	2.3	20.3	0.9
1125	312.9541194172	11728	2.6	-17.2	3.3	17.5	1.4
1126	312.6740292394	9579	1.7	-20.1	27.9	9.2	12.6
1127	313.4779607887	10984	2.0	12.2	3.6	0.3	1.8
1128	313.0522300782	12376	2.5	-13.9	7.1	-11.8	2.7
1129	313.0369728544	13107	1.7	-5.7	24.8	14.3	25.7
1130	313.0369917353	13383	1.8	-11.7	1.8	19.0	0.6
1131	313.8839970554	14115	4.7	-0.7	12.8	23.6	0.6
1132	313.8091385977	515	1.2	12.9	3.4	-20.5	34.0
1133	313.4782373420	9049	18.2	-39.5	4.4	-50.6	5.6
1134	314.0362447562	12032	0.6	-17.6	5.3	9.2	1.9
1135	314.0512215872	14206	1.3	-1.1	6.1	-4.1	4.2
1136	314.0317873456	3174	2.0	-101.5	2.2	-47.1	1.3
1137	314.6085991029	7485	1.9	-6.9	24.0	8.6	10.1
1138	314.0627063073	7790	2.1	-29.3	5.6	123.7	0.5
1139	315.6014755841	12851	1.2	-24.8	10.9	32.6	0.1
1140	315.8166166687	14369	3.0	110.7	46.6	94.0	2.6
1141	315.9718554985	3177	1.5	-91.7	8.2	-44.7	11.5
1142	315.0366028391	4789	1.5	-54.9	10.6	90.3	47.7
1143	315.8832220351	7468	1.2	-8.6	4.8	-13.8	6.4
1144	315.9514746066	748	0.3	13.8	9.6	-18.4	3.6
1145	315.8986473596	7546	2.5	-11.2	12.1	19.1	7.1
1146	316.6883170966	3177	1.4	-57.1	26.4	-51.8	4.2
1147	316.9749000892	3177	1.4	-71.9	35.2	-22.5	36.4
1148	317.8992355228	10089	1.3	-13.9	7.8	21.3	6.1
1149	317.4714387457	10998	2.5	3.1	1.1	5.7	5.2
1150	317.1181833895	3177	1.4	-74.9	1.0	-46.2	3.1
1151	318.6111844944	13591	0.8	-27.4	2.5	17.5	1.2
1152	318.4902390388	8425	3.1	-35.6	15.4	-58.0	4.9
1153	318.6198211583	8844	1.6	-12.4	1.7	16.8	2.5
1154	318.2581585855	9411	0.6	19.8	2.6	-13.9	3.1
1155	319.6211989722	11474	2.6	-10.3	0.3	18.4	2.5
1156	319.4255816558	12134	3.6	-10.6	5.2	-16.8	3.1
1157	319.6185365328	7352	1.2	-16.2	1.3	21.7	1.0
1158	320.9050917714	11844	7.9	-12.8	3.3	10.3	1.2
1159	320.0737714341	11941	1.1	-29.6	5.9	-8.3	2.8
1160	320.6107975832	11941	1.1	-23.8	6.9	14.8	2.8
1161	320.6945677553	7352	1.2	0.8	9.1	6.9	12.9
1162	320.8389675472	7354	0.8	5.3	5.9	-44.9	17.3
1163	321.0360472946	10722	2.1	-10.3	7.3	8.3	3.1
1164	321.5014708490	14191	0.2	-34.3	4.2	43.7	1.7
1165	321.4211350045	14199	1.6	3.1	12.1	-0.5	7.9
1166	321.6954809962	7000	1.4	-5.9	28.4	3.6	16.8
1167	321.8275498413	7318	0.1	-12.1	1.6	12.9	1.8
1168	322.1252073201	11240	2.3	-6.2	4.1	9.5	7.7

REFERENCES

1. J.D. Mill, R.R. O'Niel, S. Price, G.J. Romick, O.M. Vy, E.M. Gaposchkin, G.C. Light, W.W. Moore, Jr., and T.L. Murdock, "The Midcourse Space Experiment: Introduction to the spacecraft, instruments, and scientific objectives," *J. Rockets and Spacecraft,* Vol. 31, No. 5, pp. 900–907, Sept–Oct 1994.

2. *Infrared Astronomical Satellite (IRAS) Catalogs and Atlases*. Vol. I: Explanatory Supplement, Edited by C. Beichman, G. Neugebauer, H. Habing, P. Clegg, and T. Chester, Joint IRAS Science Working Group, 1984.

3. A.R.W. de Jonge, R.M. van Hess, B. Viersen, and P. Wesselius, *Detecting Space Debris Using IRAS*, Final Report and Work Packages, Groningen Space Institute, Netherlands, Document ROG-DEB-91-11, May 1991.

4. H. McCallon (at IPAC) (private communication, 1994).

5. E.M. Gaposchkin and R. Bergemann, "Infrared detections of satellites with IRAS," MIT Lincoln Laboratory, Lexington, Mass., Technical Rep. 1018 (TBD 1995).

REPORT DOCUMENTATION PAGE

Form Approved
OMB No. 0704-0188

Public reporting burden for this collection of information is estimated to average 1 hour per response, including the time for reviewing instructions, searching existing data sources, gathering and maintaining the data needed, and completing and reviewing the collection of information. Send comments regarding this burden estimate or any other aspect of this collection of information, including suggestions for reducing this burden, to Washington Headquarters Services, Directorate for Information Operations and Reports, 1215 Jefferson Davis Highway, Suite 1204, Arlington, VA 22202-4302, and to the Office of Management and Budget, Paperwork Reduction Project (0704-0188), Washington, DC 20503.

1. AGENCY USE ONLY (*Leave blank*)	2. REPORT DATE	3. REPORT TYPE AND DATES COVERED
	1 November 1995	Technical Report

4. TITLE AND SUBTITLE

A Metric Analysis of IRAS Resident Space Object Detections

5. FUNDING NUMBERS

C — F19628-95-C-0002

6. AUTHOR(S)

Mark T. Lane, Joseph F. Baldassini, and E. Michael Gaposchkin

7. PERFORMING ORGANIZATION NAME(S) AND ADDRESS(ES)

Lincoln Laboratory, MIT
244 Wood Street
Lexington, MA 02173-9108

8. PERFORMING ORGANIZATION REPORT NUMBER

TR-1022

9. SPONSORING/MONITORING AGENCY NAME(S) AND ADDRESS(ES)

BMDO/TRS
7100 Defense
The Pentagon
Washington, DC 20301-7100

10. SPONSORING/MONITORING AGENCY REPORT NUMBER

ESC-TR-95-021

11. SUPPLEMENTARY NOTES

None

12a. DISTRIBUTION/AVAILABILITY STATEMENT

Approved for public release; distribution is unlimited.

12b. DISTRIBUTION CODE

13. ABSTRACT (*Maximum 200 words*)

The Infrared Astronomy Satellite (IRAS) was launched and operated during a 10-month period in 1983. The orbit was close to the MSX orbit design, but the science data were collected in a mode where the focal plane was pointing directly away from the Earth. The Space Research Institute at Groningen, Netherlands, collected approximately 139,000 tracks of data that had focal plane motion different than astronomical sources, and the IRAS Processing and Analysis Center (IPAC) determined the boresite pointing of IRAS to within 20 arcsec. This report will focus on the nonastronomical detections from IRAS, many of which are Resident Space Objects (RSOs). In particular, the focus of the study is on how many are correlated to the known RSO catalogue for 1983 and the calibration and characterization of the metric accuracy for the correlated data. This study was undertaken to prepare for analysis of RSO detections from the MSX satellite, and in particular, so that automatic analysis tools designed for analysis of surveillance experiment data could be tested. The supporting analysis tools, required corollary data, and metric calibration procedure will be described, and the results of the accuracy of the IRAS ephemeris and metric RSO detections will be presented.

14. SUBJECT TERMS

infrared metric data
space-based observation
of artificial satellites
automatic metric processing
metric analysis
MSX
space surveillance
IRAS

15. NUMBER OF PAGES
66

16. PRICE CODE

17. SECURITY CLASSIFICATION OF REPORT	18. SECURITY CLASSIFICATION OF THIS PAGE	19. SECURITY CLASSIFICATION OF ABSTRACT	20. LIMITATION OF ABSTRACT
Unclassified	Unclassified	Unclassified	Same as Report